

MEASUREMENT OF MULTIJET CROSS-SECTION RATIOS IN PROTON-PROTON COLLISIONS WITH THE CMS DETECTOR AT THE LHC

Anterpreet Kaur

Supervisor : Prof. Manjit Kaur

Department of Physics
Panjab University
Chandigarh, India

Outline

- Physics of the Thesis
- CMS Detector
- Theoretical Background
- Analysis Strategy
- Measurement of Inclusive Multijet Cross-sections
- Theoretical Predictions
- Data-Theory Comparisons
- Cross-section Ratio R_{32}
- Determination of the Strong Coupling Constant, $\alpha_S(M_Z)$
- Summary and Outlook
- Hardware Activities

Physics of the Thesis

- The measurement of inclusive multijet event cross-sections,

$$\sigma_{i\text{-jet}} = \sigma(pp \rightarrow i \text{ jets} + X) \propto \alpha_S^i \quad * \text{to be fixed in text}$$

- ▶ and their ratio

$$R_{mn} = \frac{\sigma_m}{\sigma_n} \propto \alpha_S^{m-n}; m > n$$

- ▶ as a function of

$$\langle p_{T,1,2} \rangle = \frac{p_{T,1} + p_{T,2}}{2} = H_{T,2}/2$$

- The inclusive differential multijet event cross section is defined as :

$$\frac{d\sigma}{d(H_{T,2}/2)} = \frac{1}{\epsilon \mathcal{L}_{\text{int,eff}}} \frac{N_{\text{event}}}{\Delta(H_{T,2}/2)}, \text{ where}$$

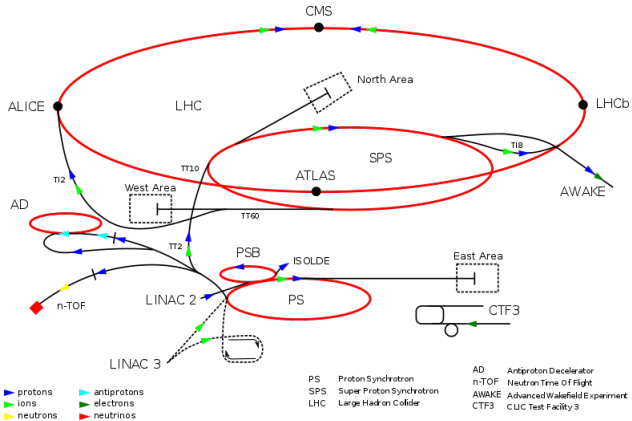
- ϵ : the product of the trigger and jet selection efficiencies and > 99%,
- $\mathcal{L}_{\text{int,eff}}$: the effective integrated luminosity,
- N_{event} : the number of 2- or 3-jet events counted in an $H_{T,2}/2$ bin, and
- $\Delta(H_{T,2}/2)$: the bin widths. The measurements are reported in units of (pb/GeV).

- In the talk :

- ▶ Highlighted text in green → changed during ARC review
- ▶ Inclusive 2-jet : $n_j \geq 2$ (300–2000 GeV), Inclusive 3-jet : $n_j \geq 3$ (300–1680 GeV),
Inclusive 4-jet : $n_j \geq 4$ (only in AN for now) and ratio : R_{32} (300–1680 GeV)

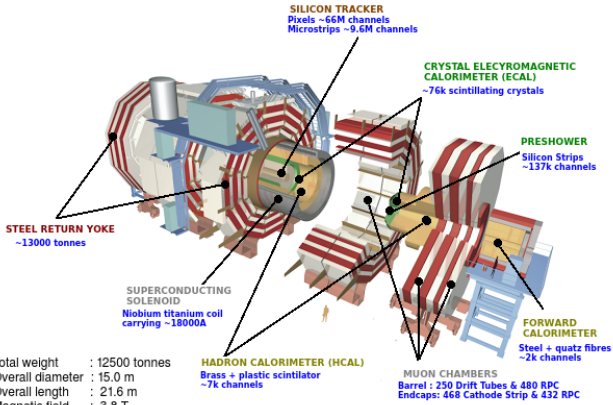
Large Hadron Collider

- World's biggest and the most powerful particle accelerator and collider built by CERN (European Organization for Nuclear Research)
- Located in a 27 km long tunnel, 100 m (approx.) underground at Swiss-France border.
- **Proton-proton (p-p),** proton-lead and lead-lead as well as xenon-xenon nuclei collisions take place at different center-of-mass energies (\sqrt{s}).
- Currently running at $\sqrt{s} = 13 \text{ TeV}$ with peak luminosity, $\mathcal{L} = 2.1 \times 10^{34} \text{ cm}^{-2} \text{ sec}^{-1}$.
- Four big experiments located at different interaction points.



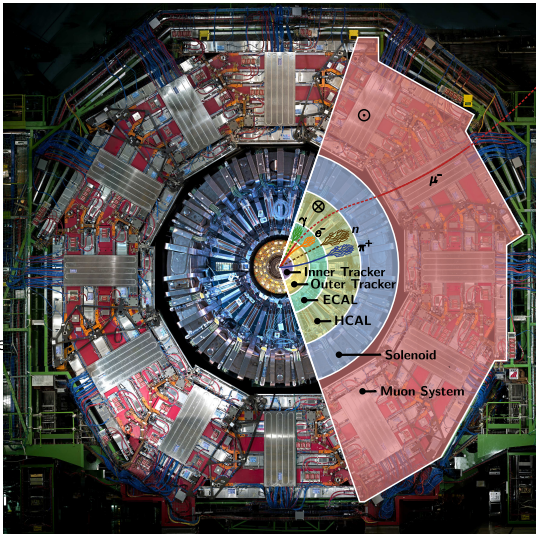
CMS Detector

- Compact Muon Solenoid (CMS) : One of the general purpose detectors which
 - is **compact** in size : 21 m long, 15 m wide and 15 m high weighing 12,500 tonnes
 - emphasis on the detection of **muons**
 - is enclosed within high **solenoidal** magnetic field
- Complex layered structure of sub-detectors : Tracker, Electromagnetic Calorimeter (ECAL), Hadron Calorimeter (HCAL) and Muon System.



CMS Detector : Front View

- Major fraction of the particles produced in p-p collisions is hadrons.
- Collimated in a given direction producing conical structures : **Jets**.
- Both hadronic (charged and neutral) and electromagnetic components.
- Charged Particles** : energy deposits in the calorimeters.
- Neutral Particles** : missing transverse energy.
- HCAL** : detects neutral particles; an essential sub-system of the CMS detector and contributes to most of physics studies with CMS.

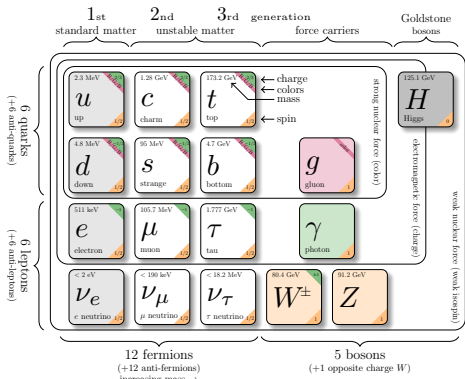


○ - Direction of magnetic field in the return yoke
⊗ - Direction of magnetic field inside the solenoid

Standard Model

- A theoretical model to describe the nature and properties of fundamental particles and their interactions.
- Fundamental particles :
 - ▶ Fermions
 - Quarks (q)
 - Leptons (ℓ)
 - ▶ Bosons
 - Gauge Bosons
 - Scalar Boson
- Forces of interactions :
 - ▶ Electromagnetic - photon (γ)
 - ▶ Strong - gluons (g)
 - ▶ Weak - W^\pm and Z
 - ▶ Gravity[★] - graviton
- Described by $SU(3)_C \otimes SU(2)_L \otimes U(1)_Y$ gauge symmetry

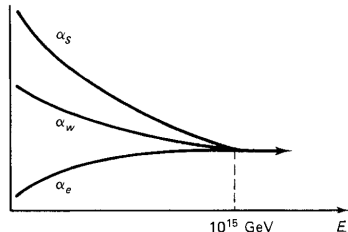
StrongElectroWeak



Quantum Chromodynamics (QCD)

- A non-abelian gauge theory describing the strong interactions between quarks and gluons.
- Color charge -
 - ▶ Quarks and gluons : colored
 - ▶ Hadrons - Baryons (qqq) and Mesons ($q\bar{q}$) : colorless
- Strong coupling constant α_S - a fundamental parameter giving the strength of interaction
- Properties -
 - ▶ Confinement : at low energies → Non-perturbative (NP) regime
 - ▶ Asymptotic freedom : at high energies → Perturbative regime
- In perturbative QCD

$$X = \sum_{i=0}^N \alpha_s^n c_i = c_0 + \alpha_s^1 c_1 + \alpha_s^2 c_2 + \dots$$

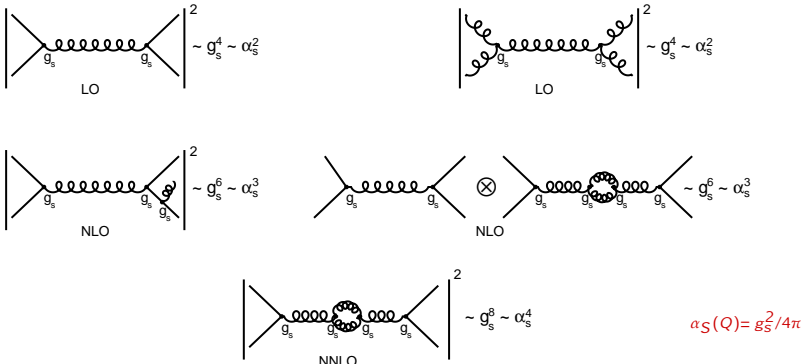


is determined by summing over the amplitudes of all Feynman diagrams.

- ▶ Power of α_S : the number of vertices associated with $q\text{-}g$ or $g\text{-}g$ interactions.

Perturbative QCD

Different orders in a $2 \rightarrow 2$ scattering process



- **Ultraviolet (UV) divergences** : Calculations become complex with the loop diagrams; associated integrals are divergent.
- **Renormalization** : a mathematical procedure which
 - ▶ allows finite calculation of momenta integrals of virtual loop by removing UV divergences
 - ▶ introduces a regulator for the infinities - **renormalization scale μ_r**
 - ▶ redefines or renormalizes the coupling constant to absorb the UV divergences

Running of the Strong Coupling

- Renormalization group equation (RGE) : exact dependence of $\alpha_S(\mu_r^2)$ on μ_r

 - Dependence of X on μ_r must cancel \rightarrow

$$\mu_r^2 \frac{d}{d\mu_r^2} X\left(\frac{Q^2}{\mu_r^2}, \alpha_s(\mu_r^2)\right) = 0$$

 - First order solution of RGE is :

$$\alpha_s(\mu_r^2) = \frac{1}{b_0 \ln(\mu_r^2/\Lambda_{QCD}^2)}$$

 - Coupling becomes large at the scale Λ_{QCD}
 - For $b_0 > 0$, coupling becomes weaker at higher scales $Q \rightarrow$ asymptotic freedom

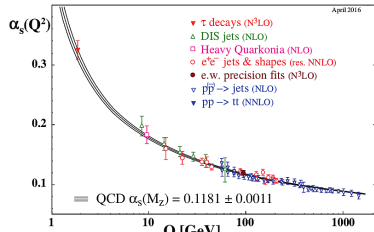
- It is always convenient to express α_S at some fixed scale -

 - Some of the best measurements come from Z decays : the strong coupling is determined at the scale of the Z boson mass $\alpha_S(M_Z)$ given by

$$\alpha_S(\mu_r, \alpha_S(M_Z)) = \frac{\alpha_S(M_Z)}{1 + \alpha_S(M_Z) b_0 \ln(\mu_r^2/M_Z^2)}$$

- α_S : a free parameter of QCD theory

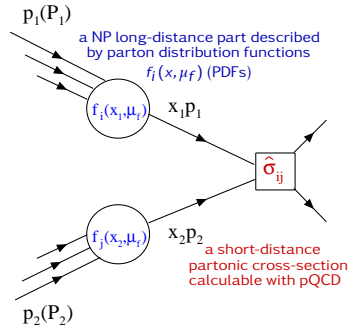
 - must be extracted from experimental measurements
 - evolved to the scale of the Z boson
 - current world average value^{*} is $\alpha_S(M_Z) = 0.1181 \pm 0.0011$



Hadronic Collisions

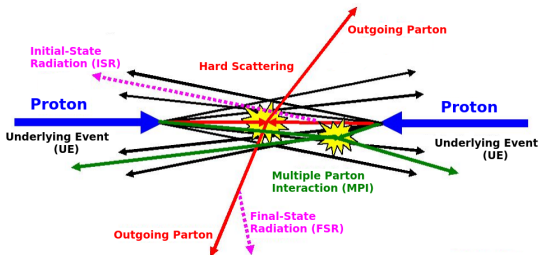
- Proton - three valence quarks (uud), gluons and the sea quarks.
- Cross-section (σ) of a certain process : the probability that the two hadrons interact and give rise to that final state.
- In a hadronic collision, the perturbation theory is only valid at the parton-level.
- **Factorization theorem** - allows the calculation of σ by separating into two parts :

$$\sigma_{P_1 P_2 \rightarrow X} = \sum_{i,j} \int dx_1 dx_2 f_{i,P_1}(x_1, \mu_f) f_{j,P_2}(x_2, \mu_f) \\ \times \hat{\sigma}_{ij} \rightarrow X \left(x_1 p_1, x_2 p_2, \alpha(\mu_r^2), \frac{Q^2}{\mu_f^2} \right)$$



- ▶ Proton PDFs f_i and f_j : probability to find a parton i with momentum fraction x within a hadron.
- ▶ Factorization scale, μ_f : corresponds to the resolution with which the hadron is being probed.
- ▶ Particles emitted with transverse momenta $p_T > \mu_f$ are considered in the calculation of hard scattering perturbative coefficients.
- ▶ Particles emitted with $p_T < \mu_f$ are accounted for within the PDFs.

Hadronic Collisions



● Hard Scattering :

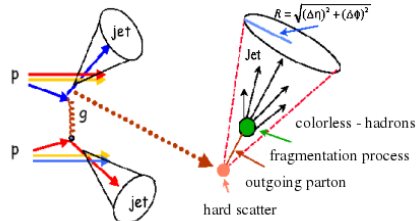
- ▶ Parton Shower : collinear parton splitting and the soft gluon emissions (pQCD).
- ▶ Hadronization : confinement of colored quarks and gluons into the color-neutral composite particles called hadrons (non-pQCD).

● Underlying Event : Event structure is significantly more complex than that of the lepton collisions.

- ▶ **Initial and Final-State Radiations (ISR, FSR)** : two incoming as well as outgoing partons can also develop parton showers.
- ▶ **Multiple Parton Interactions (MPI)** : remaining two partons which do not participate in a hard collision may also interact.

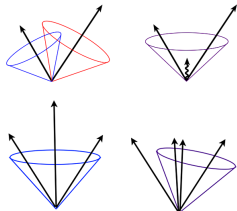
Jets

- Hadrons produced in p-p collisions get collimated in the form of conical structures called "jets".
- Direction of the jet is towards the direction of the initial partons that originated them.
- Detectable objects which relate experimental observations to theory predictions formulated in terms of partons.
- Act as a bridge between the elementary quarks and gluons of QCD and the final hadrons produced in high energy collisions.
- At the LHC, Dijet Events : $2 \rightarrow 2$, Multijet Events : $2 \rightarrow 3, 2 \rightarrow 4$
- Jets and their observables are the best tools to test the predictions of pQCD :
 - Jet production cross-section : helps to extract the value of α_S and to reduce the uncertainties of the PDFs of the proton.
 - Inclusive multijet event cross-sections permits more elaborate tests of QCD.
 - A precise study of jet variables helps to understand the signal and background modelling for new physics searches in hadronic final states.



Jet Algorithms

- Jet algorithms provide a set of rules which determine how the particles can be clustered into a jet.
- Parameters involved indicate how close two particles must be to belong to the same jet :
 - ▶ Cone algorithms → closeness in coordinate space
 - ▶ Sequential Recombination algorithms → closeness in momentum space
- Recombination Scheme
- Infrared safety : Addition of a soft emission should not change the number of hard jets found in an event.
- Collinear safety : Collinear splitting should not modify the number of jets formed in an event.
- Three types of Sequential Recombination algorithms :
 - ▶ k_t : involves clustering of soft particles first; susceptible to the underlying and pileup events
 - ▶ Cambridge/Aachen (C/A) : involves energy independent clusterings.
 - ▶ anti- k_T : cluster hard particles first; less sensitive to underlying and pileup events.



Jet Energy Corrections



- **CMSSW framework :**

- ▶ CMS software (CMSSW) includes a dedicated data structure and software tools required for data analysis.
- ▶ Performs calibration, event generation, detector simulation, event reconstruction as well as data analysis by implementing the codes either in C++ or Python languages.

- **ROOT :**

- ▶ An open source object-oriented data analysis framework.
- ▶ Consists of a huge C++ library which store and analyze large amounts of the data.
- ▶ Provides histogramming methods in 1, 2 and 3 dimensions, curve fitting functions, minimization procedures, graphics and visualization classes.

- **FASTJET :**

- ▶ a software C++ package which provides a broad range of jet finding and analysis tools in p-p and e^+e^- collisions,
- ▶ fast implementations of many sequential recombination and currently used cone algorithms
- ▶ Provides a uniform interface to external jet finders via a plug mechanism, tools for determining jet areas, to facilitate the manipulation of jet substructure, estimation of pileup and underlying-event noise levels etc.

- **NLOJET++ and FASTNLO :**

- ▶ Cross-sections for jet production at leading order (LO) and next-to-leading order (NLO) are evaluated using a C++ program called NLOJET++ FASTNLO
- ▶

Simulations and Tools



Datasets & MC Samples

● Data :

- ▶ Full 2012 dataset collected by CMS with single jet triggers
- ▶ Integrated Luminosity : 19.7 fb^{-1}

Run	Run Range	Dataset	Luminosity
A	190456-193621	/Jet/Run2012A-22Jan2013-v1/AOD	0.88 fb^{-1}
B	193834-196531	/Jet[Mon,HT]/Run2012B-22Jan2013-v1/AOD	4.49 fb^{-1}
C	198022-203742	/Jet[Mon,HT]/Run2012C-22Jan2013-v1/AOD	7.06 fb^{-1}
D	203777-208686	/Jet[Mon,HT]/Run2012D-22Jan2013-v1/AOD	7.37 fb^{-1}

- ▶ CMS software : CMSSW_5_3_11
- ▶ JECs : Winter14_V8
- ▶ Json file: Cert_190456-208686_8TeV_22Jan2013ReReco_Collisions12_JSON.txt

● Simulated Monte-Carlo (MC) Samples :

- ▶ MadGraph5+ Pythia6 TuneZ2* (MG+ P6 Z2*) :

/QCD_HT-xxxxxxxx_TuneZ2star_8TeV-madgraph-pythia6/Summer12_DR53X-PU_S10_START53_V7A-v1/AODSIM

- ▶ Herwig+ + Flat :

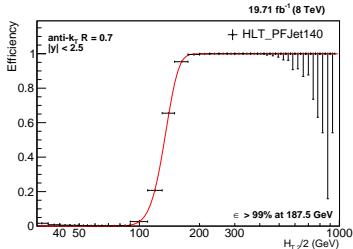
/QCD_Pt-15to3000_TuneEE3_Flat_8TeV.herwigpp/Summer12_DR53X-PU_S10_START53_V7A-v1/AODSIM

- ▶ Pythia6 Flat :

/QCD_Pt-15to3000_TuneZ2star_Flat_8TeV.pythia6/Summer12_DR53X-PU_S10_START53_V7A-v1/AODSIM

- Theoretical NLO (Next-to-leading order) calculations using the NLOJet+ + program (v4.1.3) within the framework of the fastNLO package (v2.3) using different PDF sets

- Five single-jet high-level triggers
- Only highest-threshold trigger is unprescaled
- The trigger efficiency for HLT_PFJetY is defined as :



- the value of X is chosen previous to that of Y in p_T ordering
- Z is the L1 seed value corresponding to the trigger path
- Trigger regions defined as ranges of the $H_{T,2}/2$ for every single-jet trigger used :

PAS

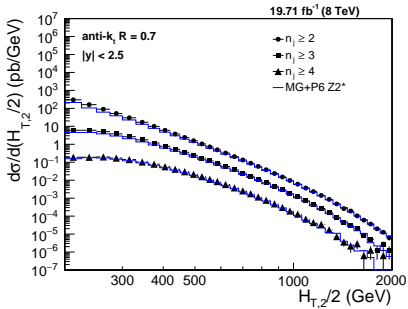
HLT path	$H_{T,2}/2$ range (GeV)	Integrated Luminosity (pb^{-1})
PF Jet80	120 – 188	212

Event Selection

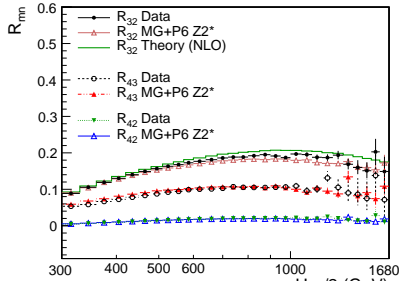
- anti- k_t particle flow (PF) jets with $R = 0.7$
- At least one good primary vertex : $|z(PV)| < 24 \text{ cm}$, $\rho(PV) < 2 \text{ cm}$, $ndof > 4$
- Tight jet ID criteria on each jet
- $p_T > 150.0 \text{ GeV}$ and $|y| < 5.0$
- Select events with at least two jets such that the two leading jets, which define $H_{T,2}/2$, have $|y| < 2.5$. Finally count all jets with $|y| < 2.5$
- $\frac{E_T^{\text{miss}}}{\sum E_T} < 0.3$ to protect against mismeasured or background events with large missing E_T

Detector Level Comparisons

- Data are compared to the sample of MG+ P6 Z2* simulated events
 - ▶ LO MC generator roughly describes the spectrum on detector level



- Cross-section ratio : $R_{mn} = \frac{\sigma_{m\text{-jet}}}{\sigma_{n\text{-jet}}}$
 - ▶ Numerator and denominator are not independent samples.
 - ▶ To calculate the statistical uncertainty before unfolding, the **Wilson score interval** is used which takes into account the correlation between the numerator and the denominator



Jet Energy Resolution (JER)

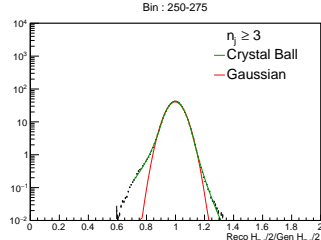
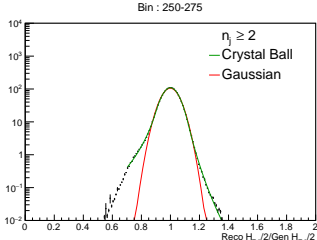
- Computed the jet energy resolution (JER) as a function of $H_{T,2}/2$ from MG+ P6 Z2* MC sample
- Measurements show that JER in data is worse than in the simulation and the jet p_T in MC need to be smeared more to describe the data
- Scaling procedure : Scaled reco jets to match resolution of data

$$p_T \rightarrow \max[0., \text{gen} + c * (p_T - \text{gen})]$$

- Non-gaussian tails are also scaled using same scaling factors determined for Gaussian core which leads to large response shifts for tails
- Smearing procedure : Smear the reconstructed jet p_T using a gaussian width widened by the scaling factor (c) (as followed in SMP-16-011)

$$p_T \rightarrow \text{Gauss}(\mu = \text{gen}, \sigma = (\sqrt{c^2 - 1}) \times \text{JER}^{\text{MC}})$$

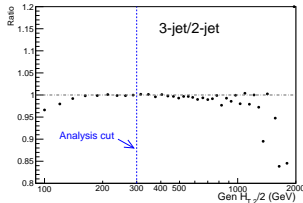
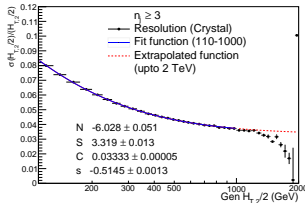
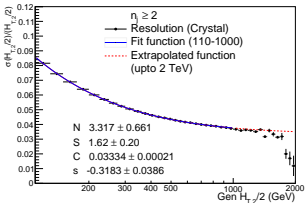
- Crystal Ball Fit of Reco $H_{T,2}/2$ / Gen $H_{T,2}/2$ in each Gen $H_{T,2}/2$ bin overlayed by Gaussian fit



Jet Energy Resolution (JER)

- Fit using NSC-formula (adapted for PF jets)
- Fits at high $H_{T,2}/2$ start lacking events

$$\frac{\sigma(x)}{x} = \sqrt{\text{sgn}(N) \cdot \frac{N^2}{x^2} + \frac{S^2}{x} \cdot x^s + C^2}$$



	N	S	C	s
Inclusive 2-jet	3.32	1.62	0.0333	-0.318
Inclusive 3-jet	-6.03	3.32	0.0333	-0.515

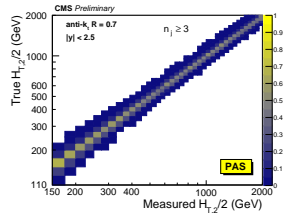
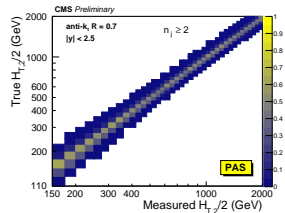
- Resolution is similar in inclusive 3-jet and 2-jet (Right Fig.)
- Fit parameters are used for smearing of NLO spectrum to construct response matrices

Unfolding

- Differential multijet cross-sections are corrected for smearing effects and unfolded to particle level
- Unfolding is performed using the iterative D'Agostini method with **4 iterations**, implemented in the RooUnfold software package
- Other number of iterations looked at (Slide no. 55 in Back-Up)
- Response matrices are shown
 - diagonal in nature, which are constructed using the Toy MC
 - Fit the NLO $H_{T,2}/2$ spectrum by the following function to obtain the true distributions (more details in Back-Up slide no. 52)

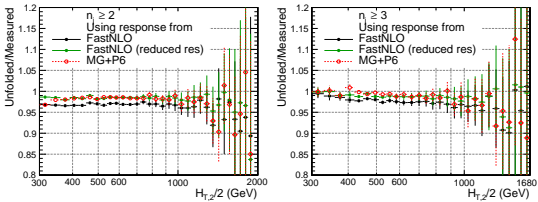
$$f(p_T) = N[x_T]^{-a} [1 - x_T]^b \times \exp[-c/x_T]$$

- The smeared distributions are generated by taking into account the additionally smeared MC resolution.
- Closure tests : small non-closures observed, accounted for additional uncertainty (more details in Back-Up slide no. 57)

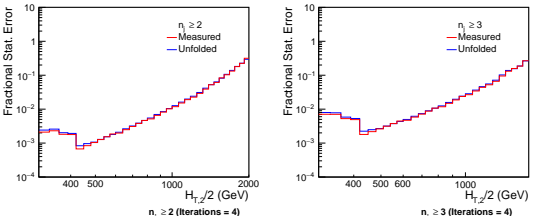


Unfolding cross-sections

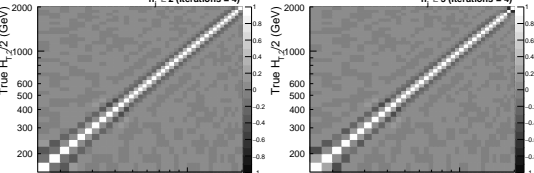
- Ratio of the unfolded data to the measured data with $H_{T,2}/2 > 300$ GeV



- Statistical errors in the unfolded distributions are slightly higher

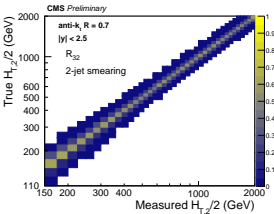
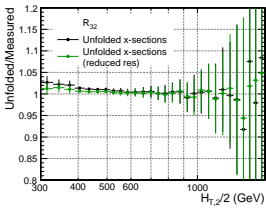


- Correlation of the statistical uncertainty introduced by the unfolding procedure

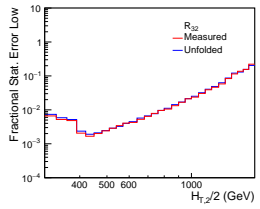
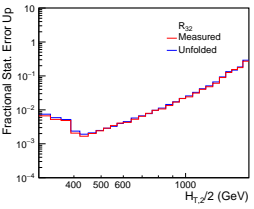


Unfolding R_{32}

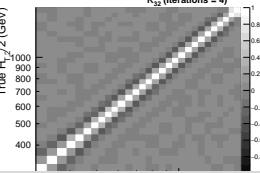
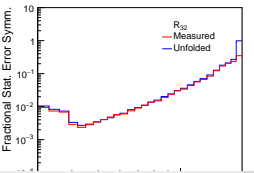
- Ratio of the unfolded cross-sections gives unfolded R_{32}



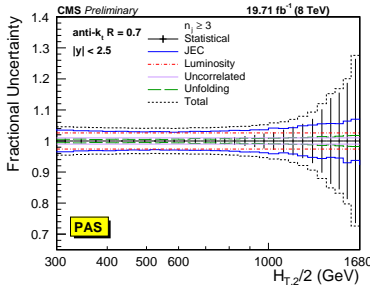
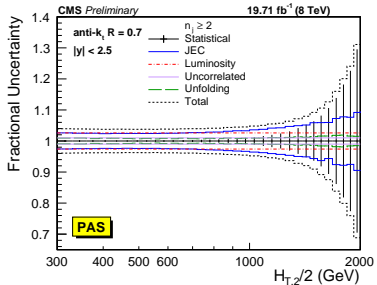
- Only to calculate the statistical correlations, R_{32} is unfolded directly using ToyMC method.



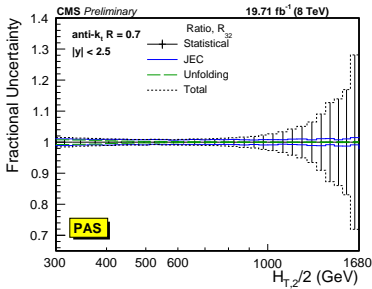
- Correlation of the statistical uncertainty introduced by the unfolding procedure



Experimental uncertainties



Uncertainty Source	Inclusive 2-jet	Inclusive 3-jet	R ₃₂
Statistical	< 1 to 30%	< 1 to 30%	< 1 to > 50%
JEC	3 to 10%	3 to 8%	1 to 2%
Unfolding	1 to 2%	1 to 2%	1%
Luminosity	2.6%	2.6%	cancels
Residual			
uncorrelated	1%	1%	cancels

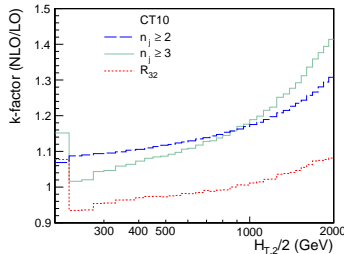


Unfolding systematic uncertainty :

- ▶ JER uncertainty : varying scale factors
- ▶ Additional uncertainty : 30% reduced resolution
- ▶ Model dependence : different functions to fit NLO predictions to obtain the true spectrum (Back Up slide no 52)

Next-to-leading order (NLO) Calculations

- The NLO theoretical calculations are done using the parton-level generator NLOJet+ within the fastNLO framework.
- The renormalization and factorization scales (μ_r and μ_f) are equal to $H_{T,2}/2$.
- Used different PDF sets (details on next slide)
- Uncertainties due to renormalization and factorization are evaluated by varying the default scale $H_{T,2}/2$ chosen for μ_r and μ_f independently in the following six combinations $(\mu_r/H_{T,2}/2, \mu_f/H_{T,2}/2) = (1/2, 1/2), (1, 1/2), (1/2, 1), (1, 2), (2, 1)$ and $(2, 2)$
- k-factor is calculated as :
$$k_{\text{fac}} = \frac{\sigma_{\text{NLO}}}{\sigma_{\text{LO}}}, k_{\text{fac}} R_{32} = \frac{k_{\text{fac}}^{\text{3-jet}}}{k_{\text{fac}}^{\text{2-jet}}}$$



- kfactor jumps at lowest $H_{T,2}/2$ for inclusive 3-jet events : Below 225 GeV some jet configurations are kinematically forbidden and the first few bins shown still suffer from these kinematical effects

Details on PDF sets

- Investigated PDF sets available via LHAPDF6

PAS

Base set	N_F	M_t (GeV)	M_Z (GeV)	$\alpha_S(M_Z)$	$\alpha_S(M_Z)$ range
ABM11	5	180	91.174	0.1180	0.110–0.130
CT10	≤ 5	172	91.188	0.1180*	0.112–0.127
MSTW2008	≤ 5	10^{10}	91.1876	0.1202	0.110–0.130
NNPDF2.3	≤ 6	175	91.1876	0.1180*	0.114–0.124
CT14	≤ 5	172	91.1876	0.1180*	0.113–0.123
HERAPDF2.0	≤ 5	173	91.1876	0.1180*	0.110–0.130
MMHT2014	≤ 5	10^{10}	91.1876	0.1180*	0.108–0.128
NNPDF3.0	≤ 5	173	91.2	0.1180*	0.115–0.121

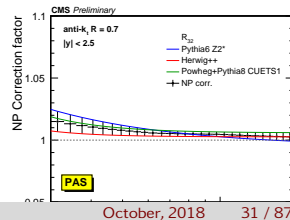
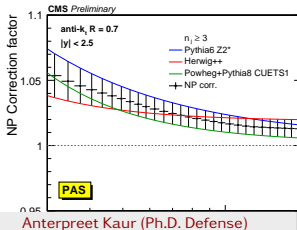
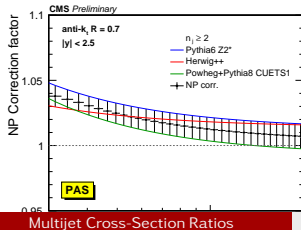
A * behind the $\alpha_S(M_Z)$ values signifies that the parameter was fixed, not fitted

- Out of these eight PDF sets the following three will not be considered further :
 - ABM11 : do not describe LHC jet data at small jet rapidity
 - HERAPDF2.0 : exclusively fits HERA DIS data with only weak constraints on the gluon PDF
 - NNPDF3.0 : the range in values available for $\alpha_S(M_Z)$ is too limited
- MSTW2008, MMHT2014 : $10^{10} \rightarrow$ Five flavours, with top quark mass \approx infinity

Non-Perturbative (NP) Corrections

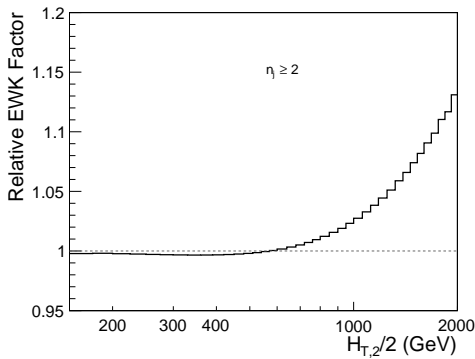
- NP corrections are required to the NLO spectrum, to compare with the experimental measurement.
 - LO generators : Pythia6 Z2* and Herwig++ (tune 2.3)
 - NLO generator : Powheg+ Pythia8 CUETS1
- NP factor is obtained by switching MPI and hadronization on/off, $c_{\text{NP}}^{\text{NP}} = \frac{\sigma^{\text{PS+ HAD+ MPI}}}{\sigma^{\text{PS}}}$
- Mean value of the envelope taken gives the NP factor and the envelope covering all differences taken as uncertainty.
- For R_{32} : first the ratio of cross sections of inclusive 3-jet to that of 2-jet events are taken separately for hadronization and MPI effects switched off and on. Then the ratio defined above is used to calculate the NP correction factor.

$$c_{R_{32}}^{\text{NP}} = \frac{\left(\frac{\sigma_{3\text{-jet}}}{\sigma_{2\text{-jet}}} \right)^{\text{PS+HAD+MPI}}}{\left(\frac{\sigma_{3\text{-jet}}}{\sigma_{2\text{-jet}}} \right)^{\text{PS}}}$$

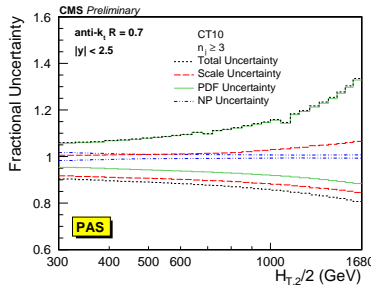
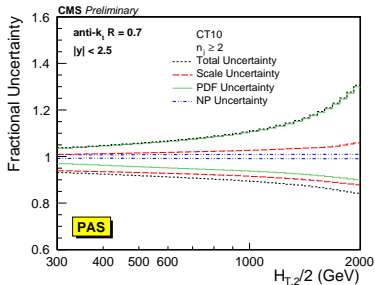


Electroweak Corrections (EWK)

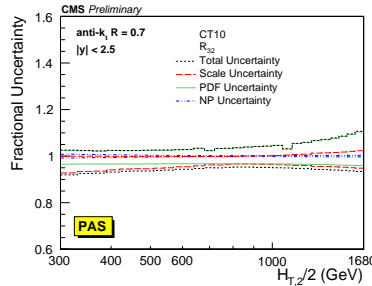
- EWK account for contributions from electroweak bosons
- Only available for inclusive 2-jet
- Best guess from theory :
 - EWK similar for inclusive 2-jet and 3-jet and hence factor of 1 for R_{32}



Theoretical Uncertainties



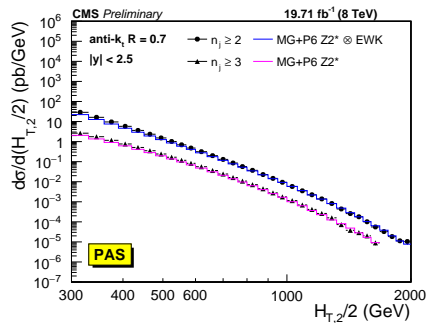
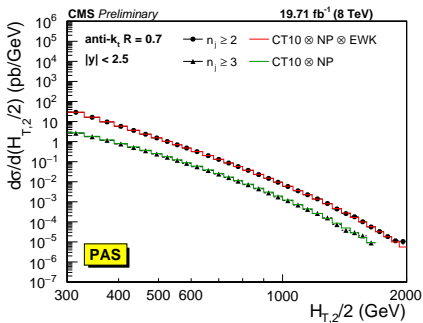
Uncertainty Source	Inclusive 2-jet	Inclusive 3-jet	R ₃₂
Scale	5 to 13%	11 to 17%	6 to 8%
PDF	2 to 30%	2 to 30%	2 to 7%
NP	4 to 5%	4 to 5%	1%



- Small dips at 1.0 TeV in the PDF uncertainty (top right): It is a feature of the CT10 PDF. Likewise the smaller dip at 700 GeV. If another PDF, e.g. CT14, is used, these dips are gone (Slide no. 65 in Back-Up).

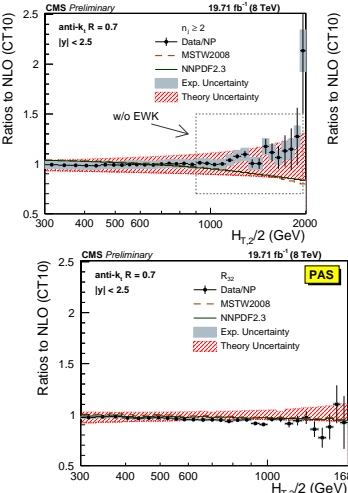
Inclusive Differential Multijet Measurement

- Inclusive differential multijet cross sections are measured as a function of the average transverse momentum, $H_{T,2}/2$
 - On Left : NLOJet+ + predictions based on the CT10 PDF set and corrected for NP effects, in addition for EWK effects in the 2-jet case
 - predictions are compatible with data within uncertainties over a wide range of $H_{T,2}/2$ from 300 GeV up to 2 TeV
 - On Right : predictions from MG+ P6 Z2*, corrected for EWK effects in the 2-jet case
 - significant discrepancies are visible in the ratio for comparison with the leading-order (LO) tree-level prediction



Comparison with NLO Predictions - CT10

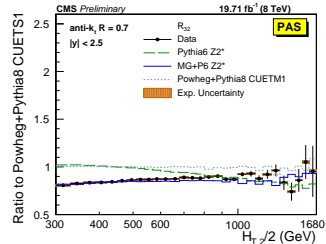
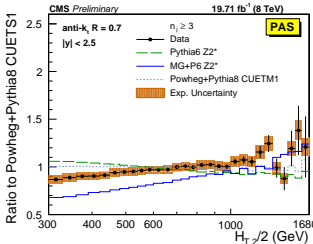
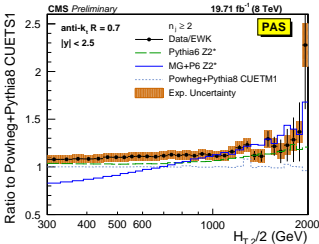
- Ratio to NLO \otimes NP \otimes EWK - CT10
- Data points with statistical uncertainty
- Theoretical uncertainty : quad. sum of scale, NP and PDF uncertainties



- Electroweak corrections explain the increasing systematic excess of data with respect to theory beyond 1 TeV of $H_{T,2}/2$ for inclusive 2-jet (Left and Middle figures)
- For brevity, the relative factor of NP between data and theory has been indicated as "Data/NP" in the legend

Comparison with MC Generators

- Ratios to Powheg+ Pythia8 tune CUETs1
- Data points with statistical uncertainty
- Experimental uncertainty shows total systematic uncertainty
- Comparison with
 - ▶ LO prediction from MG+ P6 Z2* and tree-level multi-leg improved prediction by Pythia6 Z2*: Significant discrepancies, which are cancelled to a large extent in the ratio R_{32} , are visible in particular for small $H_{T,2}/2$
 - ▶ with the matched dijet NLO prediction from Powheg+ Pythia8 with tune CUETM1 : better describes the 2-jet event cross section, but fails for the 3-jet case.

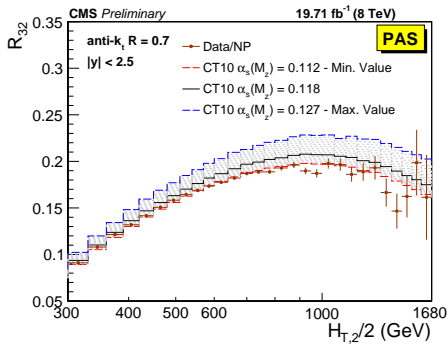


Cross section ratio (R_{32})

- The cross-section ratio R_{32} as a function of $H_{T,2}/2$ is extracted by dividing the differential cross section for inclusive 3-jet over 2-jet events for each bin in $H_{T,2}/2$

$$R_{32} = \frac{\sigma_{\text{3-jet}}}{\sigma_{\text{2-jet}}} \propto \alpha_s$$

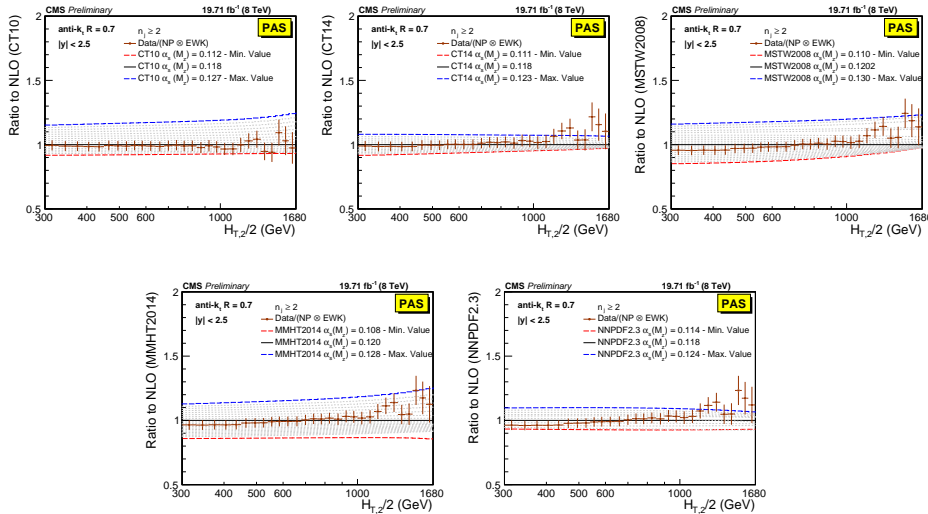
- R_{32} obtained from unfolded data in comparison to that from CT10 NLO with NP corrections. The error bars correspond to the total experimental uncertainty.



- The other ratios will also be included once the theory predictions for inclusive 4-jet events are available (for Paper).

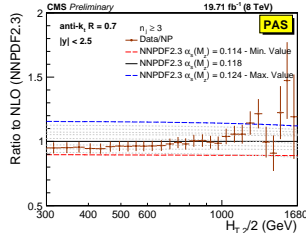
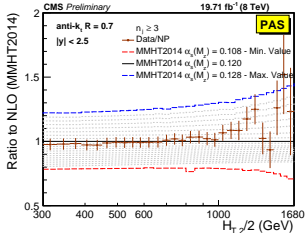
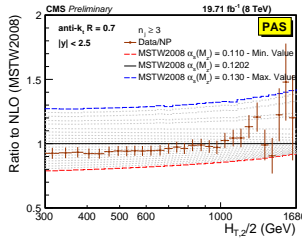
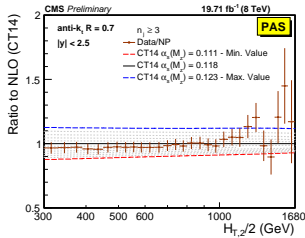
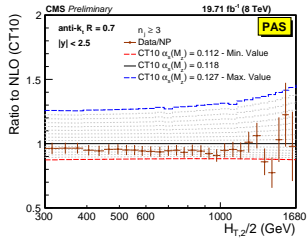
Sensitivity of differential inclusive 2-jet cross section to $\alpha_S(M_Z)$

- $\sigma_{2\text{-jet}} \propto \alpha_S^2$



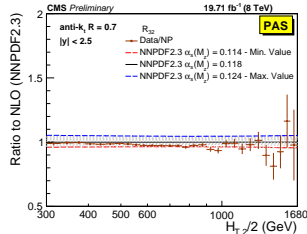
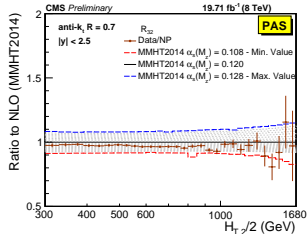
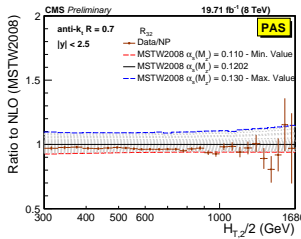
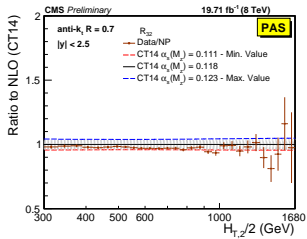
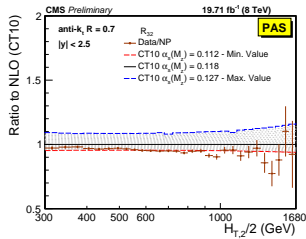
Sensitivity of differential inclusive 3-jet cross section to $\alpha_S(M_Z)$

- $\sigma_{\text{3-jet}} \propto \alpha_S^3$



Sensitivity of R_{32} to $\alpha_S(M_Z)$

- $R_{32} \propto \alpha_S^1$



Determination of the Strong Coupling Constant

- Fit of α_S using χ^2 similar to recipe as used by previous R_{32} @ 7 TeV and inclusive jets @ 8 TeV analysis

$$\chi^2 = M^T C^{-1} M$$

$$M^i = D^i - T^i$$

- $C = C_{\text{exp}} + C_{\text{theo}}$ is defined as the sum of covariances of experimental and theoretical sources of uncertainty as follows :

$$C_{\text{exp}} = \text{Cov}^{\text{ExpStat}} + \sum \text{Cov}^{\text{JEC}} + \text{Cov}^{\text{Unfolding}} + \text{Cov}^{\text{Lumi}} + \text{Cov}^{\text{Uncor}}$$

$$C_{\text{theo}} = \text{Cov}^{\text{TheoStat}} + \text{Cov}^{\text{NP}} + \text{Cov}^{\text{PDF}}$$

- $\text{Cov}^{\text{ExpStat}}$: the statistical uncertainty of the data including correlations introduced by the unfolding,
 - Cov^{JEC} : the JEC systematic uncertainty,
 - $\text{Cov}^{\text{Unfolding}}$: the unfolding systematic uncertainty including the JER,
 - Cov^{Lumi} : the luminosity uncertainty,
 - $\text{Cov}^{\text{Uncor}}$: a residual uncorrelated systematic uncertainty summarizing individual causes such as trigger and identification inefficiencies, time dependence of the jet p_T resolution, and uncertainty on the trigger prescale factors,
 - $\text{Cov}^{\text{TheoStat}}$: the statistical uncertainty caused by numerical integrations in the cross section computations,
 - Cov^{NP} : the systematic uncertainty of the NP corrections, and
 - Cov^{PDF} : the PDF uncertainty.
- For the fits of the cross sections, the range in $H_{T,2}/2$ is restricted to be between 300 GeV and 1 TeV : to avoid the region close to the minimal p_T threshold of 150 GeV for each jet at low

Fit results in range $0.3 < H_{T,2}/2 < 1.00$ TeV

PAS

PDF set	2-jets			3-jets		
	$\alpha_S(M_Z)$	$\pm \Delta \alpha_S(M_Z)$	χ^2/n_{dof}	$\alpha_S(M_Z)$	$\pm \Delta \alpha_S(M_Z)$	χ^2/n_{dof}
CT10	0.1174	0.0032	3.0/18	0.1169	0.0027	5.4/18
CT14	0.1160	0.0035	3.5/18	0.1159	0.0031	6.1/18
MSTW2008	0.1159	0.0025	5.3/18	0.1161	0.0021	6.7/18
MMHT2014	0.1165	0.0034	5.9/18	0.1166	0.0025	7.1/18
NNPDF2.3	0.1183	0.0025	9.7/18	0.1179	0.0021	9.1/18

PDF set	ignored correlations			accounted for correlations		
	$\alpha_S(M_Z)$	$\pm \Delta \alpha_S(M_Z)$	χ^2/n_{dof}	$\alpha_S(M_Z)$	$\pm \Delta \alpha_S(M_Z)$	χ^2/n_{dof}
CT10	0.1170	0.0026	8.2/37	0.1141	0.0028	19./18
CT14	0.1161	0.0029	9.1/37	0.1139	0.0032	15./18
MSTW2008	0.1161	0.0021	11./37	0.1150	0.0023	21./18
MMHT2014	0.1168	0.0025	11./37	0.1142	0.0022	19./18
NNPDF2.3	0.1188	0.0019	15./37	0.1184	0.0021	12./18

- All cross section fits give compatible values for $\alpha_S(M_Z)$ in the range of 0.115 - 0.118
- For R_{32} , smaller values are obtained as in the previous CMS R_{32} publication [Eur. Phys. J. C 73 (2013) 2604]
- small χ^2/n_{dof} except for the R_{32} fits : may be due to an overestimation of the residual uncorrelated uncertainty of 1% that is cancelled for R_{32} .
- With an assumed uncertainty of 0.25% : the χ^2/n_{dof} values lie around unity while the $\alpha_S(M_Z)$ values are still compatible with the previous results but with slightly reduced Multijet Cross-Section Ratios

Fit results in range $0.3 < H_{T,2}/2 < 1.68$ TeV

- $\alpha_S(M_Z)$ fits to the 2-jet event cross section with or without EWK correction factors.
 - ▶ Reduction in χ^2/n_{dof} indicating a better agreement when EWK effects are included.
 - ▶ A tendency to slightly smaller $\alpha_S(M_Z)$ values is observed without the EWK corrections.

PAS

PDF set	2-jets, without EWK			2-jets, with EWK		
	$\alpha_S(M_Z)$	$\pm \Delta \alpha_S(M_Z)$	χ^2/n_{dof}	$\alpha_S(M_Z)$	$\pm \Delta \alpha_S(M_Z)$	χ^2/n_{dof}
CT10	0.1163	0.0034	15./28	0.1165	0.0032	14./28
CT14	0.1137	0.0033	24./28	0.1144	0.0033	17./28
MSTW2008	0.1093	0.0028	27./28	0.1133	0.0023	19./28
MMHT2014	0.1127	0.0032	32./28	0.1141	0.0032	21./28
NNPDF2.3	0.1162	0.0024	31./28	0.1168	0.0024	23./28

- Results from the two most compatible PDF sets MSTW2008 and MMHT2014 at NLO :
 - ▶ provide a large enough range in $\alpha_S(M_Z)$ values to ensure fits without extrapolation
 - ▶ Other three PDF sets are at the limit such that reliable fits cannot be performed for estimation of all uncertainties.

PAS

PDF set	$\alpha_S(M_Z)$	$R_{32} : \Delta \alpha_S(M_Z) \times 1000$					χ^2/n_{dof}
		exp	PDF	NP	all exc. scale	scale	
MSTW2008	0.1150	± 10	± 13	± 15	± 23	$+50$ -0	26./28
MMHT2014	0.1142	± 10	± 13	± 14	± 22	$+49$ -6	24./28

Fit results in range $0.3 < H_{T,2}/2 < 1.68$ TeV

- Using R_{32} at the central scale and for the six scale factor combinations for the two PDF sets MSTW2008 and MMHT2014

PAS

$\mu_r/H_{T,2}/2$	$\mu_f/H_{T,2}/2$	MSTW2008		MMHT2014	
		$\alpha_S(M_Z)$	χ^2/n_{dof}	$\alpha_S(M_Z)$	χ^2/n_{dof}
1	1	0.1150	26./28	0.1142	24./28
1/2	1/2	0.1165	77./28	0.1160	73./28
2	2	0.1120	18./28	0.1191	18./28
1/2	1	0.1150	53./28	0.1136	48./28
1	1/2	0.1150	30./28	0.1142	28./28
1	2	0.1155	23./28	0.1147	22./28
2	1	0.1180	19./28	0.1175	19./28

- Uncertainty composition for $\alpha_S(M_Z)$ from the determination of α_S in bins of $H_{T,2}/2$

PAS

$H_{T,2}/2$ (GeV)	MSTW2008: $\Delta\alpha_S(M_Z) \times 1000$					MMHT2014: $\Delta\alpha_S(M_Z) \times 1000$				
	$\alpha_S(M_Z)$	exp	PDF	NP	scale	$\alpha_S(M_Z)$	exp	PDF	NP	scale
300–420	0.1157	± 15	± 14	± 19	$+53$ -0	0.1158	± 14	± 10	± 19	$+52$ -0
420–600	0.1153	± 11	± 14	± 18	$+57$ -0	0.1154	± 11	± 12	± 17	$+56$ -0
600–1000	0.1134	± 13	± 16	± 19	$+52$ -0	0.1140	± 12	± 12	± 18	$+45$ -0
1000–1680	0.1147	± 29	± 17	± 18	$+63$ -11	0.1154	± 25	± 14	± 15	$+56$ -11
300–1680	0.1150	± 10	± 13	± 15	$+50$ -0	0.1142	± 10	± 13	± 14	$+49$ -6

Summary

- A measurement of the inclusive 2-jet (3-jet) event cross sections has been presented in a range of $0.3 < H_{T,2}/2 < 2.0$ TeV ($0.3 < H_{T,2}/2 < 1.68$ TeV) for the average p_T of the two leading jets at central rapidity of $|y| < 2.5$
- Measured cross sections are corrected for detector effects and compared to NLO calculations
- Compared to the different PDF sets
 - ▶ Well described by calculations at NLO in pQCD complemented with NP corrections that are important at low $H_{T,2}/2$
- Compared to the different Monte Carlo generators
 - ▶ LO tree-level MC predictions exhibit significant deviations.
- $\alpha_S(M_Z)$ Determination
 - ▶ Performed fits of $\alpha_S(M_Z)$ from differential inclusive 2-jet and inclusive 3-jet event cross-sections separately and in combined fit as well as ratio R_{32} , in the range in $H_{T,2}/2$ of 0.3 TeV up to 1.00 TeV.
 - ▶ MSTW2008 and MMHT2014 PDF sets provide a large enough range in $\alpha_S(M_Z)$ values and give similar results in full range in $H_{T,2}/2$ of 0.3 TeV up to 1.68 TeV and for scale variations in this range, and also for subranges in $H_{T,2}/2$
 - ▶ Using MSTW2008 PDF set, the strong coupling constant is determined in a fit to the R_{32} measurement to :

$$\begin{aligned}\alpha_S(M_Z) &= 0.1150 \pm 0.0010 (\text{exp}) \pm 0.0013 (\text{PDF}) \pm 0.0015 (\text{NP})^{+0.0050}_{-0.0000} (\text{scale}) \\ &= 0.1150 \pm 0.0023 (\text{all except scale})^{+0.0050}_{-0.0000} (\text{scale})\end{aligned}$$

- ▶ Agreement with the world average value of $\alpha_S(M_Z) = 0.1181 \pm 0.0011$

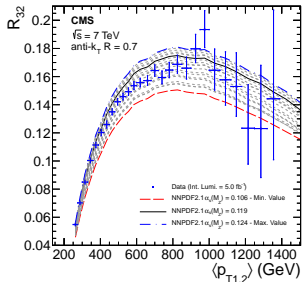
We kindly request for the approval of this analysis. Thank you !!

Back-Up Slides

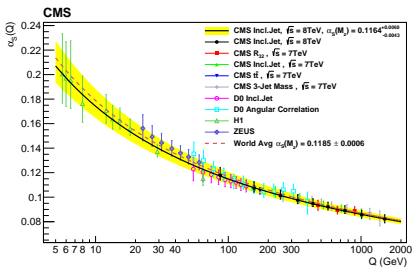
Sequential Recombination Algorithms

- Based on transverse momentum p_T of the particles.
 1. Distance d_{ij} between two particles i and j and distance d_{iB} of the particle to the beam are calculated as
$$d_{ij} = \min(p_{Ti}^{2p}, p_{Tj}^{2p}) \frac{\Delta R_{ij}^2}{R^2}, \quad d_{iB} = p_{Ti}^{2p}$$
where $\Delta R_{ij}^2 = (y_i - y_j)^2 + (\phi_i - \phi_j)^2$
 2. If $d_{ij} < d_{iB}$, particles i and j are merged into a new single jet object k , summing four-momenta of two initial particles by recombination scheme and step 1 is repeated.
 3. If $d_{iB} < d_{ij}$, particle i is declared as a final-state jet and the particle gets removed from the list.
- Value of the parameter p defines the three different sequential algorithms :
 - ▶ k_t algorithm : $p = 1$
 - ▶ Cambridge/Aachen (C/A) algorithm : $p = 0$
 - ▶ anti- k_T algorithm : $p = -1$

Previous Results



- Ratio of inclusive 3- to 2-jet events = $\frac{\sigma_{3\text{-jet}}}{\sigma_{2\text{-jet}}}$
 $\propto \alpha_S$ vs $\langle p_{T1,2} \rangle$ at $\sqrt{s} = 7$ TeV
- Comparison with NLO calculations
- $\alpha_S(M_Z) = 0.1148 \pm 0.0014$ (exp.) ± 0.0018 (PDF) ± 0.0050 (theory) = **0.1148 ± 0.0055**
- **7 TeV Published**
- **Eur. Phys. J. C 73 (2013) 2604**



- Measurement and QCD analysis of double-differential inclusive jet cross-sections in pp collisions at $\sqrt{s} = 8$ TeV and ratios to 2.76 and 7 TeV
- $\alpha_S(M_Z)$ (NLO) = $0.1164^{+0.0025}_{-0.0029}$ (PDF)
 $+ 0.0053$ (Scale) ± 0.0001 (NP) $^{+0.0014}_{-0.0015}$ (Exp) = **$0.1164^{+0.0060}_{-0.0043}$**
- **8 TeV Submitted**
- **arXiv:1609.05331**

Introduction

- The measurement of inclusive multijet event cross-sections,

$$\sigma_{i\text{-jet}} = \sigma(pp \rightarrow i \text{ jets} + X) \propto \alpha_S^i \quad * \text{to be fixed in text}$$

- ▶ and their ratio

$$R_{mn} = \frac{\sigma_m}{\sigma_n} \propto \alpha_S^{m-n}; m > n$$

- ▶ as a function of

$$\langle p_{T,1,2} \rangle = \frac{p_{T,1} + p_{T,2}}{2} = H_{T,2}/2$$

- The inclusive differential multijet event cross section is defined as :

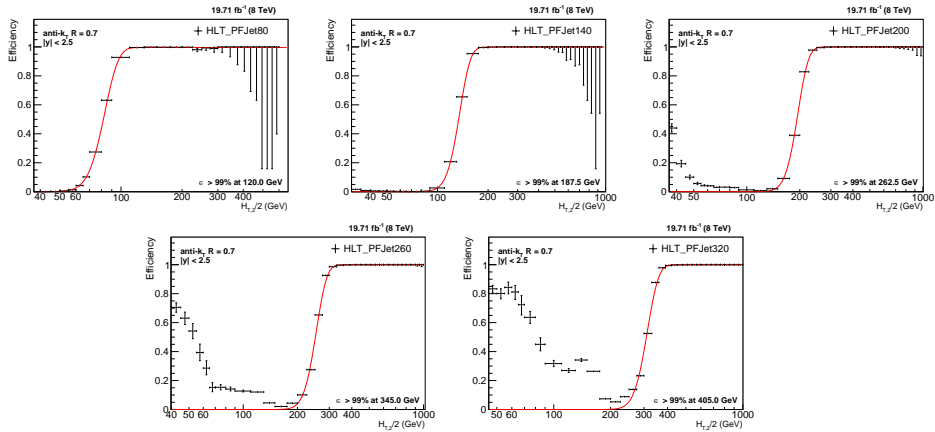
$$\frac{d\sigma}{d(H_{T,2}/2)} = \frac{1}{\epsilon \mathcal{L}_{\text{int,eff}}} \frac{N_{\text{event}}}{\Delta(H_{T,2}/2)}, \text{ where}$$

- ϵ : the product of the trigger and jet selection efficiencies and > 99%,
- $\mathcal{L}_{\text{int,eff}}$: the effective integrated luminosity,
- N_{event} : the number of 2- or 3-jet events counted in an $H_{T,2}/2$ bin, and
- $\Delta(H_{T,2}/2)$: the bin widths. The measurements are reported in units of (pb/GeV).

- The measured cross-section is corrected for detector effects and is compared to the NLO \otimes NP QCD predictions for different PDF sets
- Fits of the strong coupling constant are performed for inclusive 2-jet and 3-jet event cross-sections separately and for their ratio R_{32}
- In the talk :

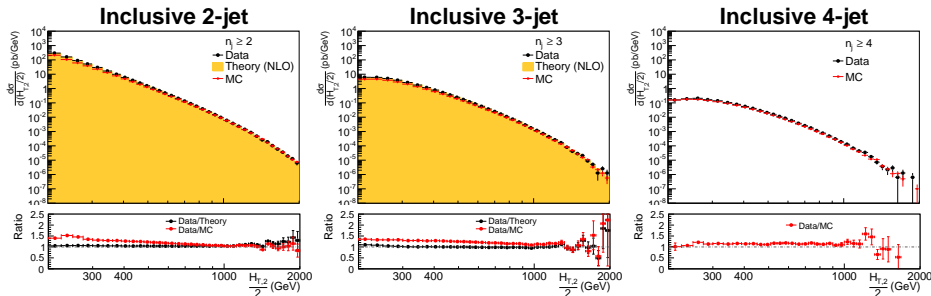
- ▶ Highlighted text in green → changed during ARC review
- ▶ Inclusive 2-jet : $n_j \geq 2$ (300–2000 GeV), Inclusive 3-jet : $n_j \geq 3$ (300–1680 GeV),
Inclusive 4-jet : $n_j \geq 4$ (only in AN for now) and ratio : R_{32} (300–1680 GeV)

Trigger Efficiencies vs $H_{T,2}/2$



Detector-Level Comparison of Cross Sections

- Binning used is inherited from R₃₂ at 7 TeV : 150., 175., 200., 225., 250., 275., 300., 330., 360., 390., 420., 450., 480., 510., 540., 570., 600., 640., 680., 720., 760., 800., 850., 900., 950., 1000., 1060., 1120., 1180., 1250., 1320., 1390., 1460., 1530., 1600., 1680., 1760., 1840., 1920., 2000.
- Comparison of 2012 full data is done with NLO predictions as well as MG+ P6 MC Simulations.
- 150-200 bins are not included to avoid the infrared sensitivity for the bins next to min. p_T cut in NLO calculations for events with inclusive 2-jet events.



★ NLO theory predictions are yet to be done for inclusive 4-jet events.

Unfolding : Fitting NLO predictions

- Fitting the NLO $H_{T,2}/2$ spectrum by the function ([Function I](#))

$$f(p_T) = N[x_T]^{-a} [1 - x_T]^b \times \exp[-c/x_T]$$

where N is normalization factor and a, b, c are fit parameters.

- ▶ This function is derived from the below function from “**Measurement of the Inclusive Jet Cross Section in pp Collisions at $\sqrt{s}=7$ TeV**” ([Phys.Rev.Lett. 107, 132001 \(2011\)](#))

$$f(p_T; \alpha, \beta, \gamma) = N_0[p_T]^{-a} [1 - \frac{1}{\sqrt{s}} 2p_T \cosh(y_{\min})]^{\beta} \times \exp[-\gamma/p_T], \text{ where } N_0 \text{ is a normalization factor, } \alpha, \beta, \gamma \text{ are fit parameters, and } y_{\min} \text{ is the low-edge of the rapidity bin } y \text{ under consideration.}$$

using

$$\alpha = a, \beta = b, \gamma = c * \sqrt{s}/2,$$

$$x_T = \frac{2*p_T*cosh(y_{\min})}{\sqrt{s}} = \frac{2*p_T}{\sqrt{s}}$$

where transverse scaling variable x_T corresponds to the proton fractional momentum x for dijets with rapidity $y=0$,

$\sqrt{s} = 8000$ GeV and y_{\min} is low-edge of the rapidity bin y under consideration (Here y_{\min} is taken equal to 0)

- Fitting the NLO $H_{T,2}/2$ spectrum by the function ([Function II](#)) ([CMS AN-12-223](#)):

$$f(H_{T,2}/2) = A_0 \left(1 - \frac{H_{T,2}/2}{A_6}\right)^{A_7} \times 10^F(x), \text{ where } F(x) = \sum_{i=1}^5 A_i \left(\log\left(\frac{x}{A_6}\right)\right)^i$$

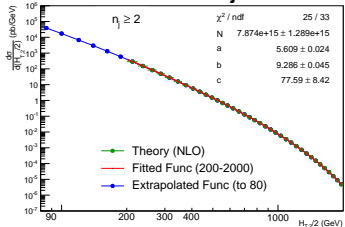
where the parameter A_6 is fixed to $\frac{\sqrt{s}}{2\cosh(y_{\min})}$, where $\sqrt{s} = 8000$ GeV and y_{\min} is the minimum rapidity. The other parameters are derived from the fitting.

Unfolding : Fitting NLO predictions

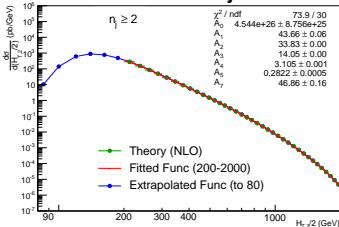
- First fit the NLO spectrum with function in the range (specified on the plot) and then using the obtained fit parameters extrapolated it to lower value.

Function I (Left) and Function II (Right)

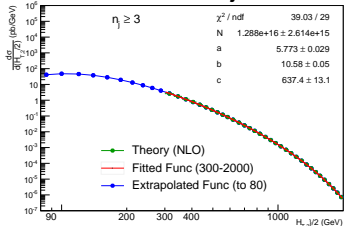
Inclusive 2-jet



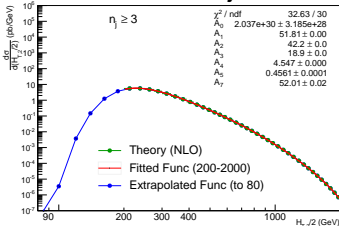
Inclusive 2-jet



Inclusive 3-jet

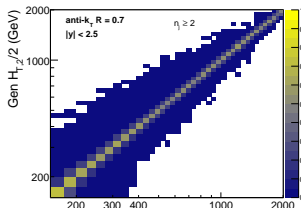


Inclusive 3-jet

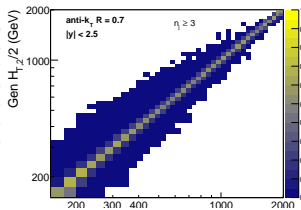


Unfolding (from MG+ P6)

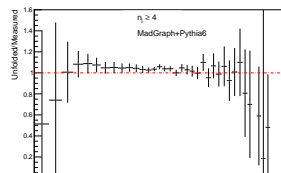
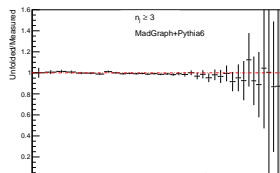
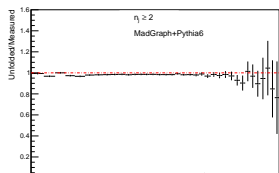
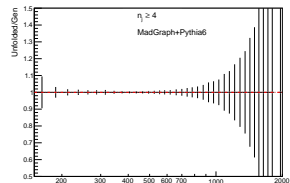
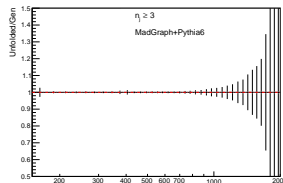
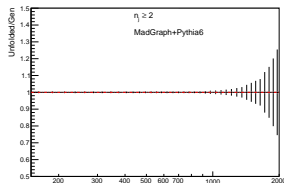
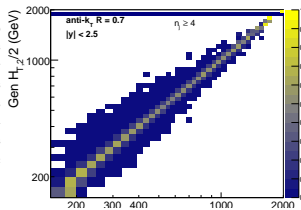
Inclusive-2 jet



Inclusive-3 jet

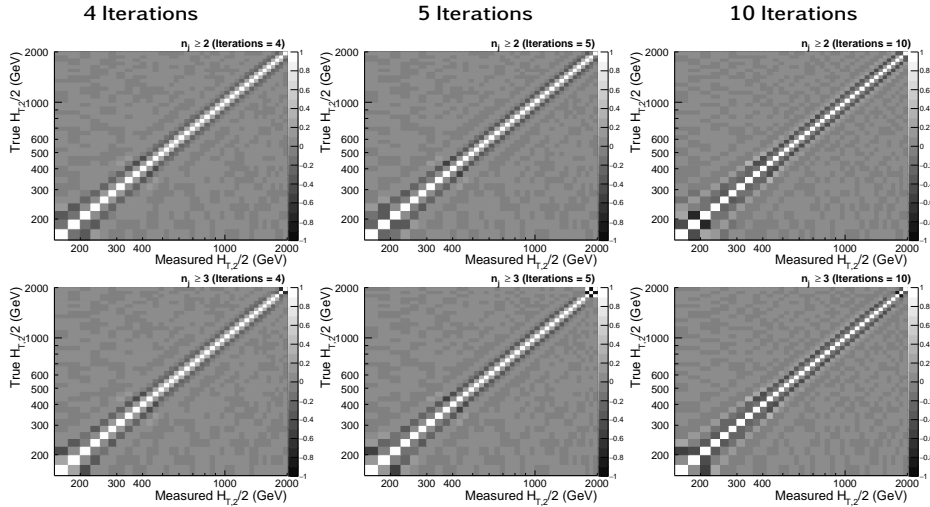


Inclusive 4-jet

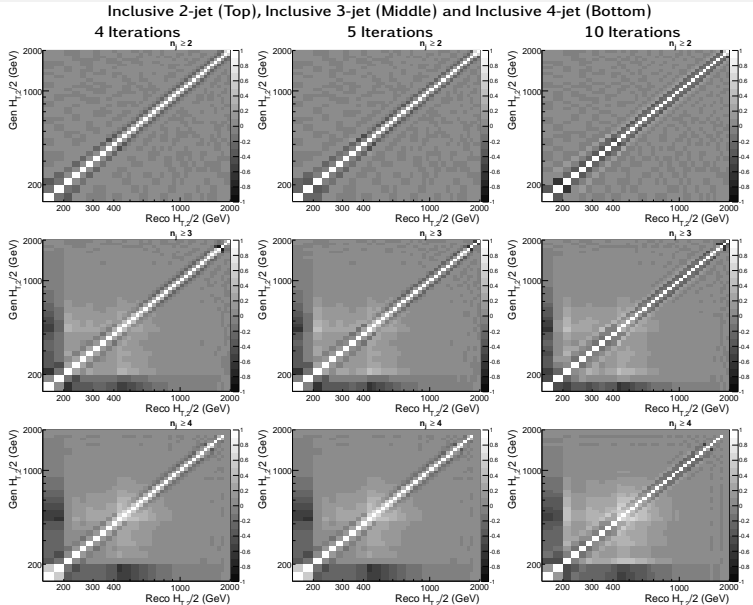


Unfolding : Correlation Matrices (NLO)

Inclusive 2-jet (Top) and Inclusive 3-jet (Bottom)



Unfolding : Correlation Matrices (MG+ P6)



Closure tests

Blue curve

- ▶ Simulated MG+ P6 Reco/MG+ P6 Gen
- ▶ Resolution (Res.) is extracted from this simulation

Red curve

- ▶ Extracted Res. smears FastNLO too much, in a very large y bin
- ▶ ARC agreed to add this non-closure as additional uncertainty for now

Black dashed curve

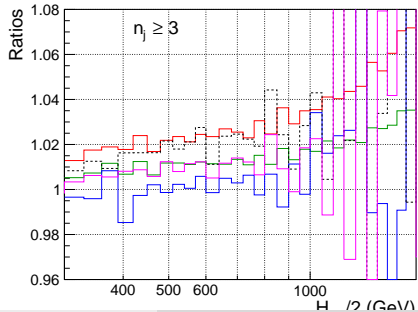
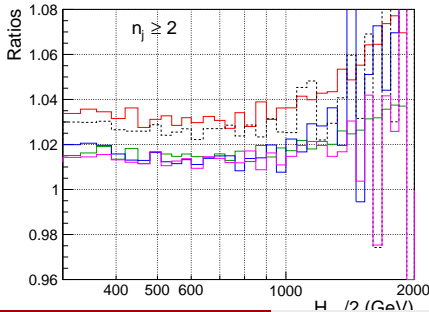
- ▶ Proves that the extracted Res. also smears MG+ P6 Gen more

Magenta curve

- ▶ Closure with **blue curve** when 30% reduced Res. is used to smear MG+ P6 Gen

Green curve

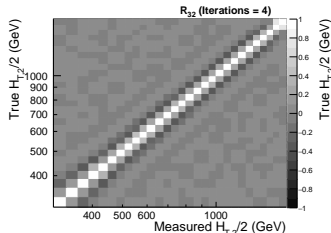
- ▶ Closure with **blue curve** when FastNLO is smeared using 30% reduced Res.
- ▶ An additional uncertainty is attributed by comparison to an unfolding with a 30% reduced Res. with the one using extracted Res.



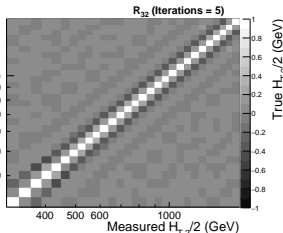
Unfolding R_{32}

Correlation Matrices (NLO)

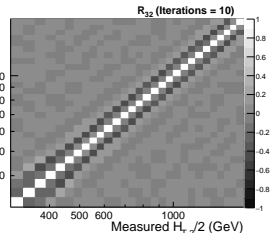
4 Iterations



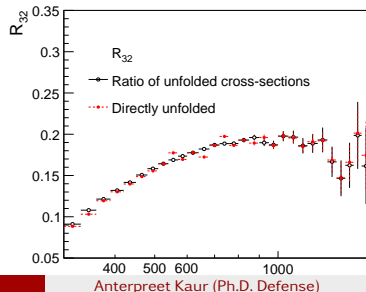
5 Iterations



10 Iterations



Unfolding R_{32}



JES Uncertainty in $\frac{H_{T,2}}{2}$

● Jet Energy Scale (JES)

- ▶ 24 JES mutually uncorrelated uncertainty sources (Winter14_V8) are considered :
 - AbsoluteStat, AbsoluteScale, AbsoluteMPFBias,
 - Fragmentation, SinglePionECAL, SinglePionHCAL, FlavorQCD,
 - RelativeJEREC1, RelativeJEREC2, RelativeJERHF, RelativePtBB, RelativePtEC1, RelativePtEC2, RelativePtHF, RelativeFSR, RelativeStatFSR, RelativeStateEC2, RelativeStatHF,
 - PileUpDataMC, PileUpPtRef, PileUpPtBB, PileUpPtEC1, PileUpPtEC2, PileUpPtHF
- ▶ Relative uncertainties for **AbsoluteFlavMap, RelativeJERHF, RelativePtHF, RelativeStatHF, PileUpPtHF** are exactly zero

● To get uncertainty in P_T for each source :

double unc = Event→pfjet(p).uncSrc(isrc); where p is jet and isrc is uncertainty source

● Calculated $P_T^{up} = (1 + unc) * P_T$ and $P_T^{down} = (1 - unc) * P_T$ for each source (Event wise)

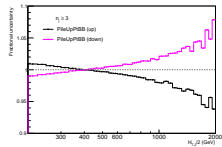
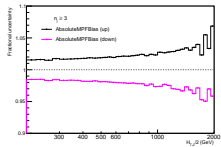
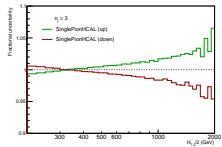
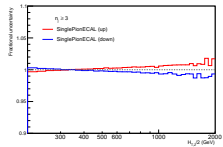
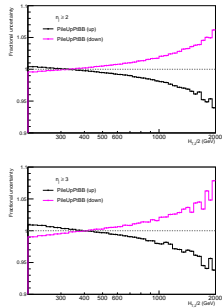
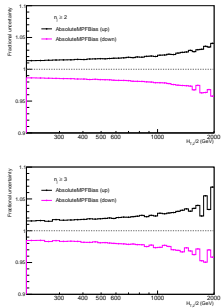
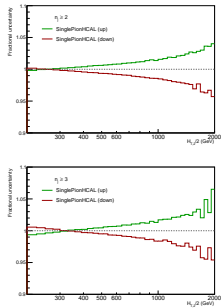
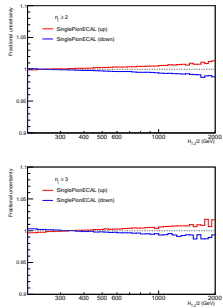
● Calculated $\frac{H_{T,2}}{2} = \frac{\sum_{i=1}^2 P_{T,i}}{2}$ and $\frac{H_{T,2}^{up}}{2} = \frac{\sum_{i=1}^2 P_{T,i}^{up}}{2}$, $\frac{H_{T,2}^{down}}{2} = \frac{\sum_{i=1}^2 P_{T,i}^{down}}{2}$ for each source (Event wise) and filled in histograms

● After filling histograms, calculated average uncertainty (%) in $\frac{H_{T,2}}{2}$, for each source :

$$\left(\frac{\frac{H_{T,2}^{up}}{2} - \frac{H_{T,2}^{down}}{2}}{2 * \frac{H_{T,2}}{2}} \right) * 100$$

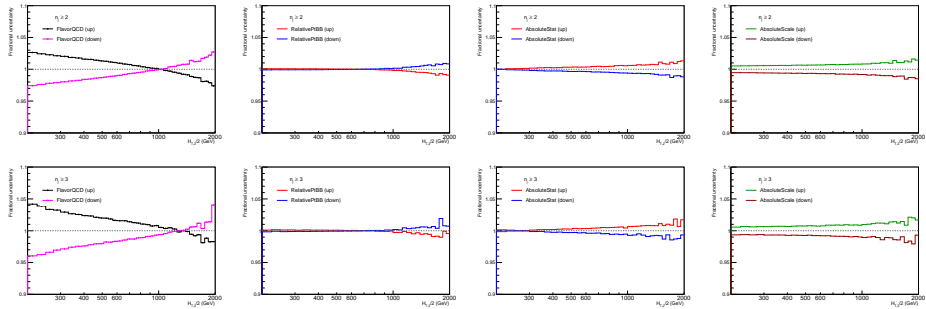
JES Uncertainty in $H_{T,2}/2$ (Single)

Inclusive 2-jet (Top) and Inclusive 3-jet (Bottom)



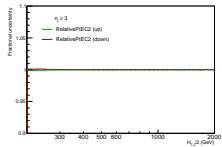
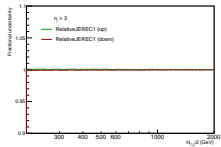
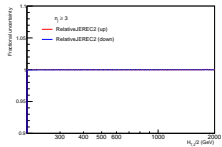
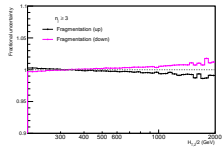
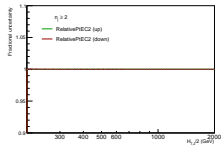
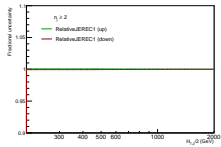
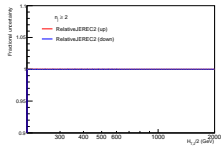
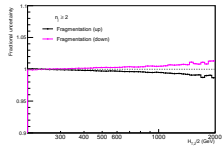
JES Uncertainty in $H_{T,2}/2$ (Single)

Inclusive 2-jet (Top) and Inclusive 3-jet (Bottom)



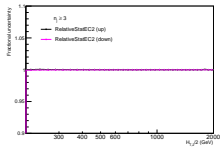
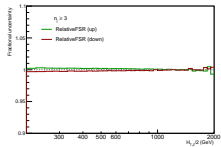
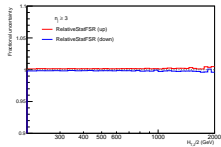
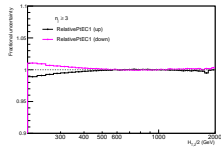
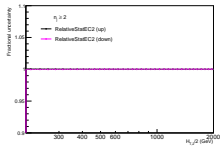
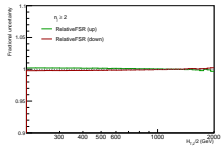
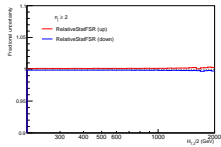
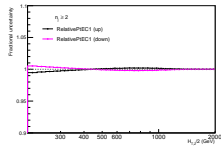
JES Uncertainty in $H_{T,2}/2$ (Single)

Inclusive 2-jet (Top) and Inclusive 3-jet (Bottom)



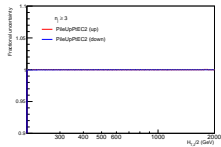
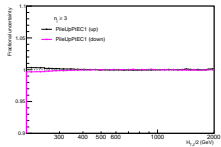
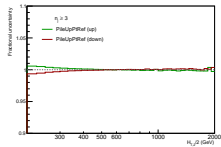
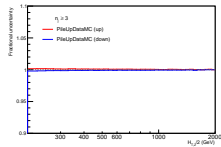
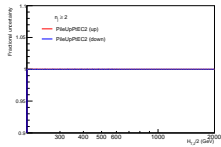
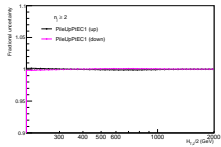
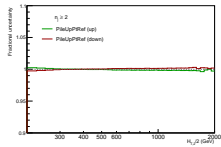
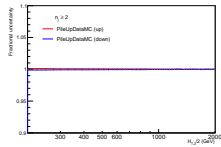
JES Uncertainty in $H_{T,2}/2$ (Single)

Inclusive 2-jet (Top) and Inclusive 3-jet (Bottom)

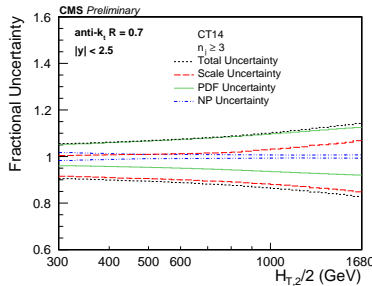
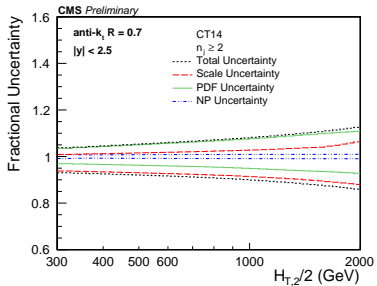


JES Uncertainty in $H_{T,2}/2$ (Single)

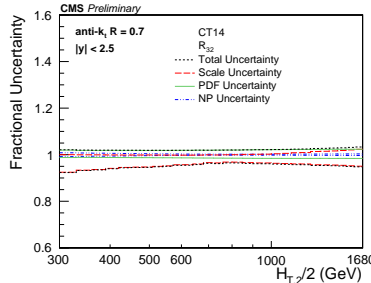
Inclusive 2-jet (Top) and Inclusive 3-jet (Bottom)



Theoretical Uncertainties (CT14)



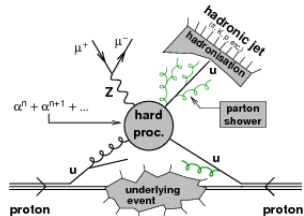
Uncertainty Source	Inclusive 2-jet	Inclusive 3-jet	R ₃₂
Scale	5 to 13%	11 to 17%	6 to 8%
PDF	2 to 10%	5 to 11%	2 to 3%
NP	4 to 5%	4 to 5%	1%



Introduction

Jets :

- key component to extend our understanding of the Standard Model physics
- signatures of large momentum transfers at short distances, belong primarily to perturbative domain of Quantum Chromodynamics (pQCD)
- produced abundantly in the collisions of protons at the Large Hadron Collider (LHC)
- important backgrounds for many new physics models

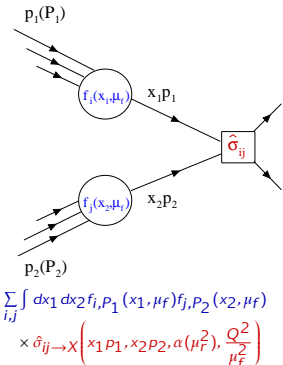


Inclusive jet cross section measurement :

- gives important information about the strong coupling constant α_S

$$\sigma_{i\text{-jet}} = \sigma(pp \rightarrow i \text{ jets} + X) \propto \alpha_S^i$$

- provides a deep insight to understand the proton structure by deriving constraints on the parton distribution functions (PDFs)

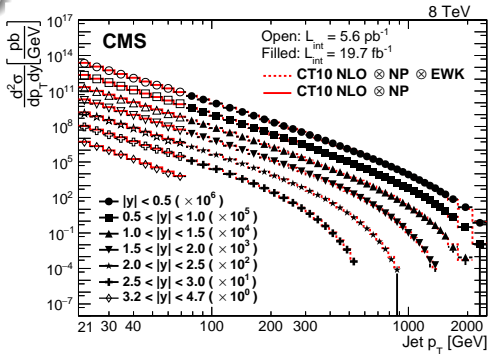


Inclusive jet production @ 8 TeV

Double-differential cross-section

$$\frac{d^2\sigma}{dp_T dy} = \frac{1}{\epsilon \mathcal{L}_{int,eff}} \frac{N_{jets}}{\Delta p_T (2\Delta|y|)}$$

- Measurement at 8 TeV
 $\mathcal{L} = 19.7 \text{ fb}^{-1}$ and $\mathcal{L} = 5.6 \text{ pb}^{-1}$
- anti- k_t jets with $R = 0.7$
- $21 \leq < 74 \text{ GeV}$, upto $|y| = 4.7$
 $74 \leq < 2500 \text{ GeV}$, upto $|y| = 3.0$
- Theoretical NLO calculations :
 - using CT10 PDF set
 - corrected for non-perturbative (NP) and electroweak (EWK) effects



JHEP 03 (2017) 156

Inclusive jet production @ 8 TeV

Data/theory using the CT10 NLO PDF :

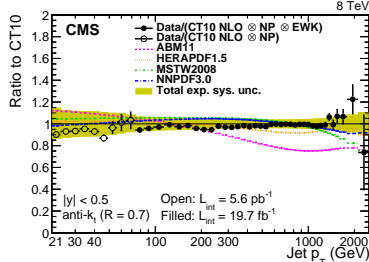
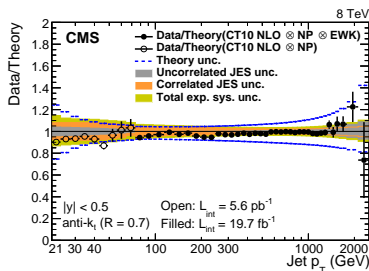
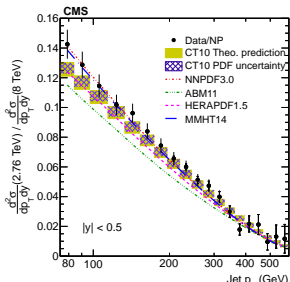
- Good agreement except low-region
- Data uncertainties : jet energy scale (1-45%), lumi (2.6%)
- NLO uncertainties : scale (5-40%), PDF (10-100%)

Ratios to CT10 PDF :

- Significant discrepancies with ABM11 PDF

Ratios 2.76/8 TeV, 7/8 TeV :

- Partial reduction of uncertainties → better sensitivity to PDFs

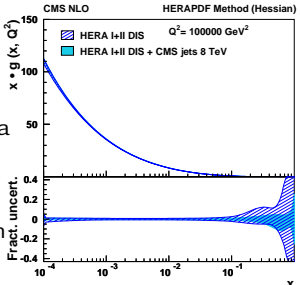


JHEP 03 (2017) 156

Inclusive jet production @ 8 TeV

QCD analysis using HeraFitter (1.1.1)

- Inclusive cross sections + HERA inclusive DIS :
 - ▶ probes hadronic parton-parton interaction over a wide range of x and Q
 - ▶ constraints on PDFs
 - ▶ significant improvement of the gluon distribution



Extraction of α_S

- Least square minimization on $p_T(y)$ spectrum :
 - ▶ using the CT10 NLO PDF set

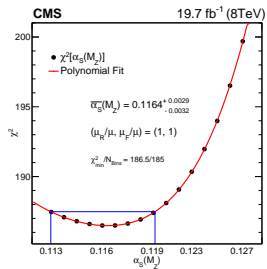
$$\alpha_S(M_Z) = 0.1164^{+0.0060}_{-0.0043}$$

- using the NNPDF3.0 NLO PDF set

$$\alpha_S(M_Z) = 0.1172^{+0.0083}_{-0.0075}$$

- Consistent with the world average value :

$$\alpha_S(M_Z) = 0.1181 \pm 0.0011$$



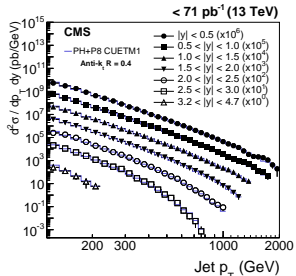
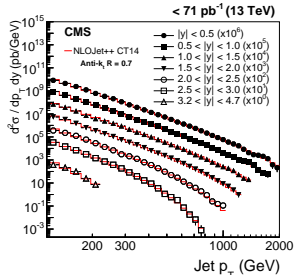
JHEP 03 (2017) 156

Inclusive jet production @ 13 TeV

Double-differential cross-section

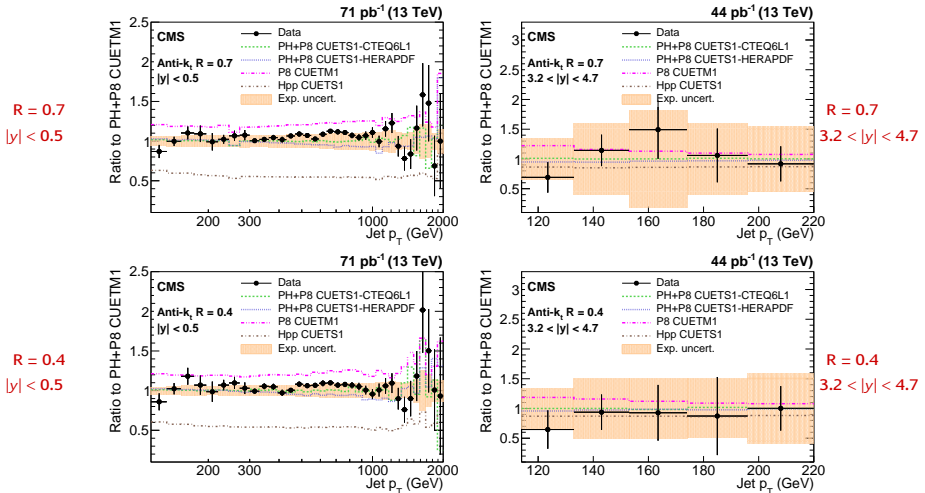
$$\frac{d^2\sigma}{dp_T dy} = \frac{1}{\epsilon \mathcal{L}_{\text{int,eff}}} \frac{N_j}{\Delta p_T \Delta y}$$

- Measurement at 13 TeV
 $\mathcal{L} = 71 \text{ pb}^{-1}$ and $\mathcal{L} = 44 \text{ pb}^{-1}$
- anti- k_t jets with $R = 0.4$ and $R = 0.7$
- $< 2 \text{ TeV}$
- Large rapidity coverage : $|y| < 3$, $3.2 < |y| < 4.7$
- Theoretical NLO calculations :
 - using CT14 PDF set
 - corrected for non-perturbative (NP) and electroweak (EWK) effects
- x-sections accurately described for $R = 0.7$, while for $R = 0.4$ theory overestimates by 5–10%



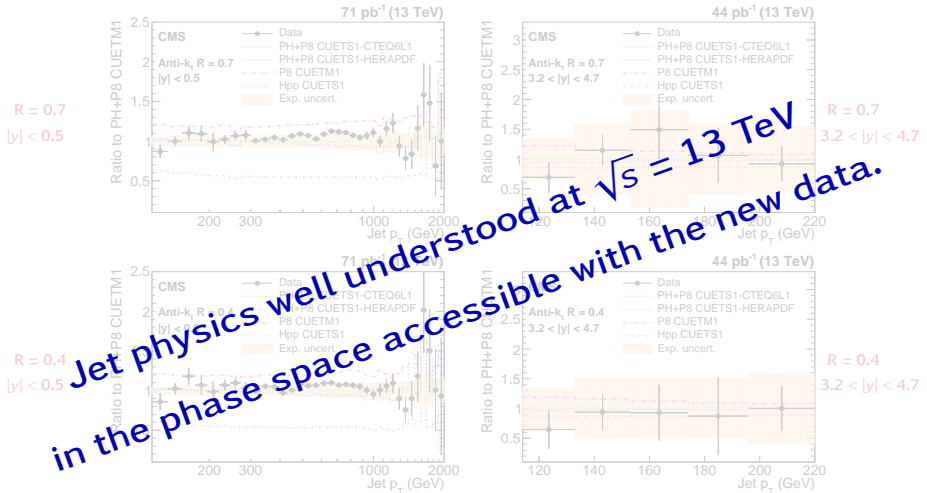
EPJC 76 (2016) 451

Inclusive jet production @ 13 TeV



- PYTHIA8 CUETM1 (LO) agrees well in shape for only $|y| < 1.5$.
- HERWIG++ CUETS1 (LO) agrees in shape for all rapidity bins.
- POWHEG+PYTHIA8 (NLO) with various tunes show good agreement for both R.

Inclusive jet production @ 13 TeV



- PYTHIA8 CUETM1 (LO) agrees well in shape for only $|y| < 1.5$.
- HERWIG++ CUETS1 (LO) agrees in shape for all rapidity bins.
- POWHEG+PYTHIA8 (NLO) with various tunes show good agreement for both R.

Triple-Differential dijets

Triple differential cross-section

$$\frac{d^3\sigma}{dp_{T,\text{avg}} dy^* dy_b} = \frac{1}{\epsilon \mathcal{L}_{\text{int}}^{\text{eff}}} \frac{N}{\Delta p_{T,\text{avg}} \Delta y^* \Delta y_b}$$

- Measurement at 8 TeV, $\mathcal{L} = 19.7 \text{ fb}^{-1}$

- anti- k_t jets with $R = 0.7$

- Cross section as a function of the :

- ▶ average transverse momentum,

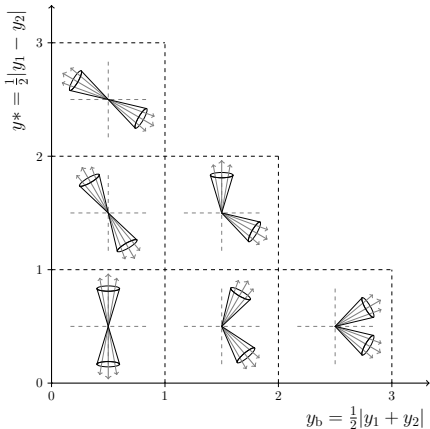
$$p_{T,\text{avg}} = \frac{1}{2}(p_{T,1} + p_{T,2})$$

- ▶ half the rapidity separation,

$$y^* = \frac{1}{2}|y_1 - y_2|$$

- ▶ boost of the two leading jets,

$$y_b = \frac{1}{2}|y_1 + y_2|$$



EPJC 77 (2017) 746

Triple-Differential dijets

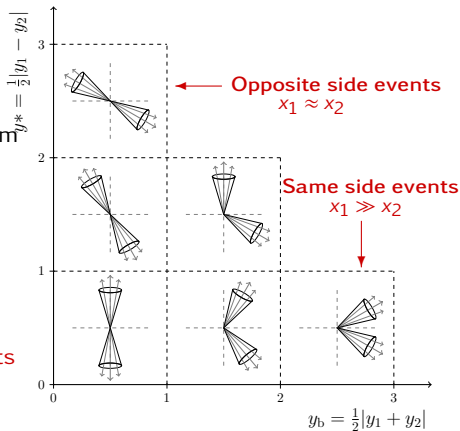
Triple differential cross-section

$$\frac{d^3\sigma}{dp_{T,\text{avg}} dy^* dy_b} = \frac{1}{\epsilon \mathcal{L}_{\text{int}}^{\text{eff}}} \frac{N}{\Delta p_{T,\text{avg}} \Delta y^* \Delta y_b}$$

- Dijet rapidities and the parton momentum fractions are related :

$$x_{1,2} = \frac{p_T}{\sqrt{s}} (e^{\pm y_1} + e^{\pm y_2})$$

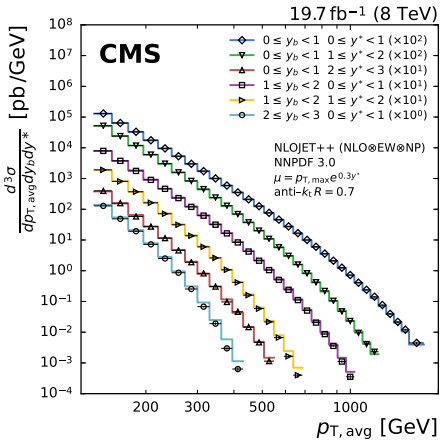
- For small y_b , $x_1 \approx x_2 \rightarrow$ Opposite side events
- For large y_b , $x_1 \gg x_2 \rightarrow$ Same side events
(Boosted region)



EPJC 77 (2017) 746

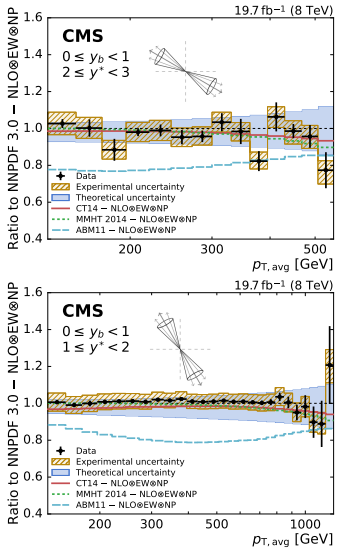
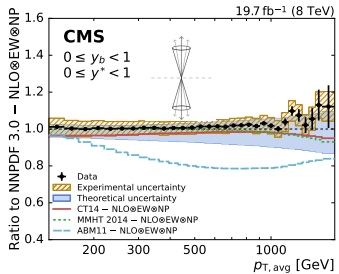
Triple-Differential dijets

- $p_{T,\text{avg}}$ spectrum for six phase-space regions in y^* and y_b
- Theoretical NLO predictions :
 - ▶ using NLOJET++ with NNPDF 3.0 PDF set
 - ▶ corrected for non-perturbative (NP) and electroweak (EW) effects
- Data are well described by NLO predictions except for the boosted region.



Triple-Differential dijets

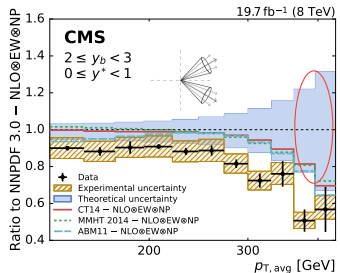
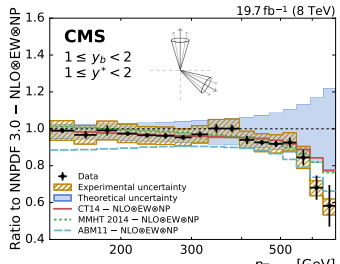
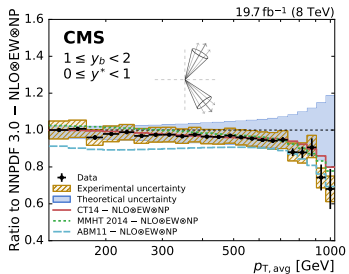
- Ratios to NNPDF 3.0 - NLO \otimes EW \otimes NP
- Data points with statistical uncertainty
- Experimental uncertainty
- Theoretical uncertainty (PDF, Scale and NP)
- Good agreement with MMHT2014 and CT14 PDF NLO calculations
- ABM11 PDF underestimates the predictions



EPJC 77 (2017) 746

Triple-Differential dijets

- Data are well described in most of the analysed phase spaces.
- Differences observed at high $p_{T,\text{avg}}$ and y_b : less known high x region of the PDFs is probed.
- Smaller data uncertainties : potential to constrain the PDFs.



Triple-Differential dijets

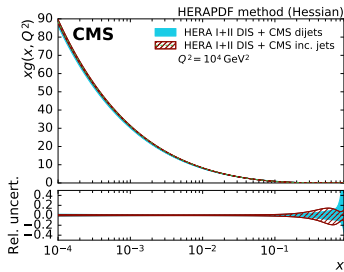
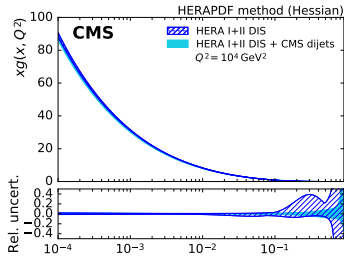
QCD analysis using XFitter (1.2.2)

- Dijet cross sections + HERA inclusive DIS :
 - ▶ an increased gluon PDF at high x with reduced uncertainties of the PDFs
 - ▶ change in shape especially at low Q^2
- Comparison of gluon PDFs with inclusive jet data :
 - ▶ similar shapes of the PDFs and the uncertainties
- Precise α_S extraction together with PDF fit :

$$\alpha_S(M_Z) = 0.1199 \pm 0.0015 (\text{exp})^{+0.0031}_{-0.0020} (\text{theo})$$

- Agreement with the world average value :

$$\alpha_S(M_Z) = 0.1181 \pm 0.0011$$



Inclusive multijets

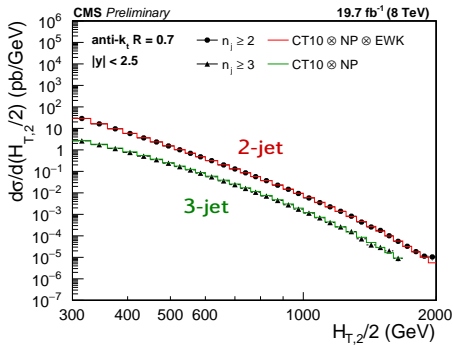
Differential cross-section

$$\frac{d\sigma}{d(H_{T,2}/2)} = \frac{1}{\epsilon \mathcal{L}_{int,eff}} \frac{N_{event}}{\Delta(H_{T,2}/2)}$$

- Measurement at 8 TeV, $\mathcal{L} = 19.7 \text{ fb}^{-1}$
- anti- k_t jets with $R = 0.7$
- 2-jet and 3-jet event cross sections as a function of :

$$H_{T,2}/2 = \frac{1}{2}(p_{T,1} + p_{T,2})$$

- Theoretical NLO calculations :
 - using CT10 PDF set
 - corrected for non-perturbative (NP) and electroweak (EWK) effects



CMS-PAS-SMP-16-008

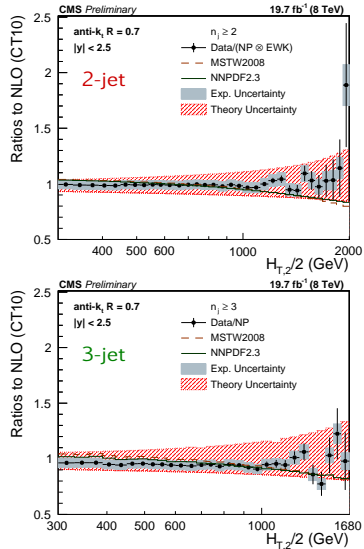
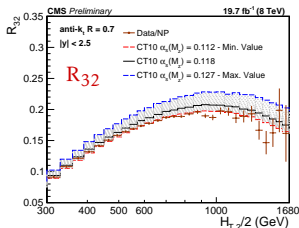
Inclusive multijets

Multijet cross sections

- Data are well described by theory predictions within uncertainty.
- EWK corrections explain the increasing excess of the 2-jet data w.r.t. theory (~ 1 TeV).

Cross section ratio

- $R_{32} = \frac{\sigma_{3\text{-jet}}}{\sigma_{2\text{-jet}}} \sim \alpha_S$
- Experimental uncertainties, theory uncertainties due to NP effects, PDFs, scale choice, EWK corrections may cancel partially or fully
- Better tool to extract α_S

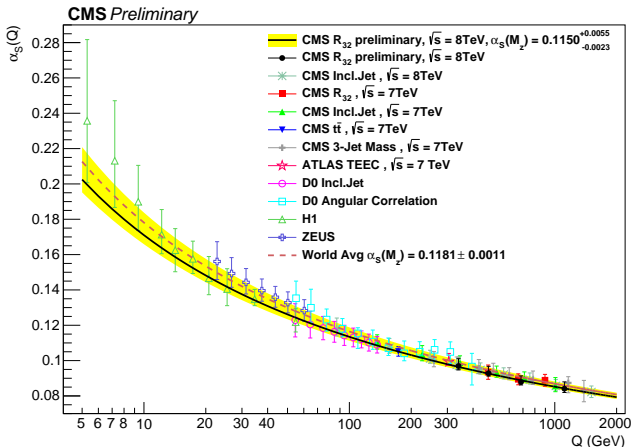


CMS-PAS-SMP-16-008

Inclusive multijets

Determination of α_S

- By minimizing the χ^2 between the measurement and the theory
- In a fit to R_{32} , using the MSTW2008 PDF set : $\alpha_S(M_Z) = 0.1150 \pm 0.0023$ (all except scale) $^{+0.0050}_{-0.0000}$ (scale)
- $\alpha_S(M_Z)$ extracted in ranges of $H_{T,2}/2 \rightarrow$ evolved to $\alpha_S(Q)$

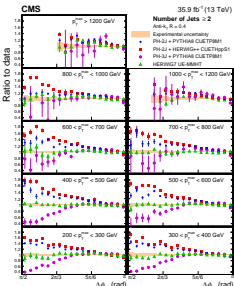
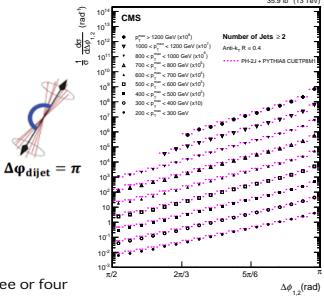


Azimuthal correlations

Normalized differential cross-section

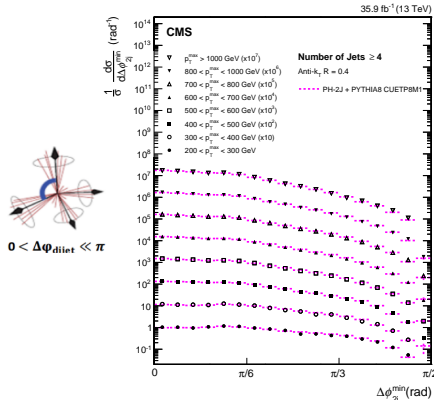
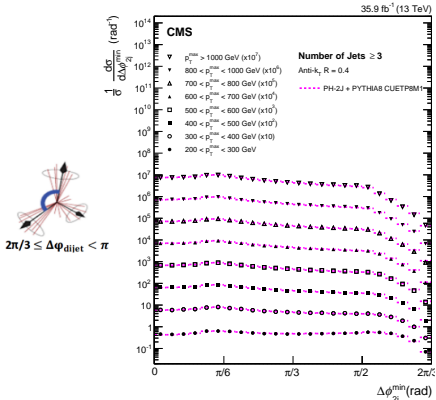
$$\frac{1}{\sigma} \frac{d\sigma}{d\Delta\phi_{1,2}}, \quad \frac{1}{\sigma} \frac{d\sigma}{d\Delta\phi_{2j}^{\min}} \text{ (3-jet and 4-jet)}$$

- Measurement at 13 TeV, $\mathcal{L} = 35.9 \text{ fb}^{-1}$
- anti- k_t jets with $R = 0.4$
- Normalized cross sections as a function of the :
 - azimuthal angular separation between the two highest leading jets
 - minimum azimuthal angular separation between any two of the three or four leading jets (3-jet and 4-jet)
- Spectrum gets flatter and become more sensitive to parton shower on moving from 2-jet to 3-jet to 4-jet
- Best agreement is given by Herwig7
- POWHEG-2J gives better results when matched with Pythia8 than Herwig++
- POWHEG-3J+Pythia8 is generally lower than POWHEG-2J+Pythia8



arXiv:1712.05471 (Submitted to EPJC)

Azimuthal correlations



- Pythia8 (LO) exhibits small deviations from the $\Delta\phi_{1,2}$ and fails to describe $\Delta\phi_{2j}^{\text{min}}$
- Herwig++ exhibits the largest deviations from the $\Delta\phi_{1,2}$ but provides a reasonable description of the $\Delta\phi_{2j}^{\text{min}}$
- MADGRAPH+Pythia8 provides a good overall description of the measurements except for $\Delta\phi_{2j}^{\text{min}}$ in 4-jet case
- An interesting tool to test the theoretical predictions of multijet production processes

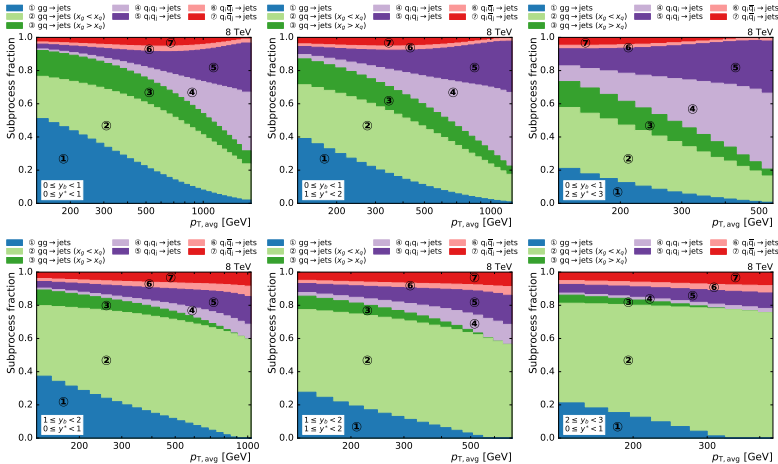
Summary

- Jet production in pp collisions is one of the main phenomenological predictions of pQCD.
- Many interesting results from CMS[★], reaching new levels of precision and exploring new regions of phase space :
 - ▶ Measurements of differential jet cross sections over a wide range in transverse momenta from inclusive jets to multi-jet final states are presented.
 - ▶ Compared to theoretical predictions including those matched to parton shower and hadronization.
 - ▶ Impact on the determination of the strong coupling constant α_S as well as on parton density functions (PDFs) are reported.
- Wide range of jet measurements at various collision energies improve our understanding of QCD.

THANKS!!

Back-Up Slides

Triple-differential dijets

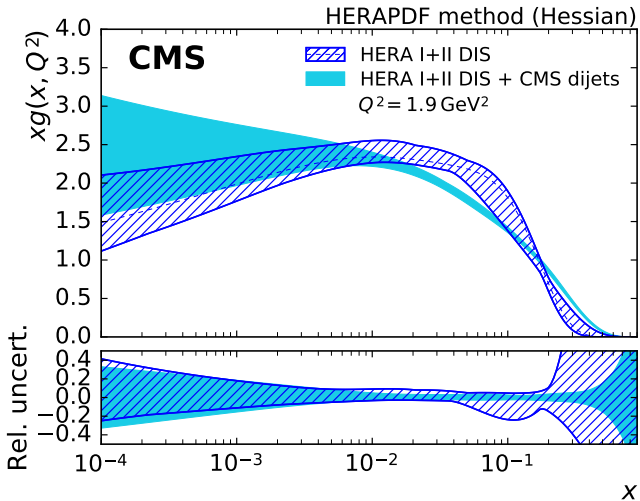


Triple-differential dijets

Data set	n_{data}	HERA data		HERA & CMS data	
		χ^2_{P}	$\chi^2_{\text{P}}/n_{\text{data}}$	χ^2_{P}	$\chi^2_{\text{P}}/n_{\text{data}}$
NC HERA-I+II e^+p $E_p = 920 \text{ GeV}$	332	382.44	1.15	406.45	1.22
NC HERA-I+II e^+p $E_p = 820 \text{ GeV}$	63	60.62	0.96	61.01	0.97
NC HERA-I+II e^+p $E_p = 575 \text{ GeV}$	234	196.40	0.84	197.56	0.84
NC HERA-I+II e^+p $E_p = 460 \text{ GeV}$	187	204.42	1.09	205.50	1.10
NC HERA-I+II e^-p	159	217.27	1.37	219.17	1.38
CC HERA-I+II e^+p	39	43.26	1.11	42.29	1.08
CC HERA-I+II e^-p	42	49.11	1.17	55.35	1.32
CMS triple-differential dijet	122	—	—	111.13	0.91
Data set(s)	n_{dof}	χ^2	χ^2/n_{dof}	χ^2	χ^2/n_{dof}
HERA data	1040	1211.00	1.16	—	—
HERA & CMS data	1162	—	—	1372.52	1.18

EPJC 77 (2017) 746

Triple-differential dijets



EPJC 77 (2017) 746